

POLITECNICO DI TORINO
Facoltà di Ingegneria
Corso di Laurea in Ingegneria Elettrica

Tesi di Laurea Magistrale

**Virtual Design and optimization of PM Motors
for Application to an Electric Vehicle**



Relatore:

Prof. Gianmario Pellegrino

Candidato:

Leonardo Ferretti

07 Ottobre 2019

To Pietro 01/09/2019

It is our choices, Harry,
that show what we truly are,
far more than our abilities.

Abstract

Traction motors play a critical role in electrified vehicles including electric, hybrid electric, and plug-in hybrid electric vehicles. With high efficiency and power density, interior permanent magnet (IPM) synchronous machines have been employed in many commercialized electrified powertrains.

In this thesis, three different IPM rotor design configurations, are comparatively investigated.

Each topology is redesigned and improved to meet new design requirements based on the same constraints. The designed motors are then compared and comprehensively evaluated for motor/vehicle performance.

Acknowledgement

I would like to thank my supervisor and examiner Prof. Gianmario Pellegrino for his endless commitment to give vital support, feedback, and encouragement.

I also wish to express my gratitude to Dr Raf Schuermans, Senior Manager at Toyota Motor Europe for his suggestions and help to this work in all possible aspects.

Additionally, I am very grateful for all of the friendly colleagues at the Politecnico of Torino, at Toyota Motor Europe and at the Université libre de Bruxelles which together contribute to a very pleasant journey.

Finally, I give my warmest thanks to my family whose support after all is the most essential.

Leonardo Ferretti

Torino, Italia

September , 2019

Contents

Acknowledgement	6
List of figures.....	10
Chapter 1: Introduction and objective of research.....	13
1.1. Introduction	13
1.2. About Motor-CAD	15
1.3. Motivation and research objectives	16
1.4. Toyota Motor Europe.....	16
1.4.1. Toyota Motor Europe.....	17
1.4.2. Subsidiaries and related company.....	19
Chapter 2: Battery Electric vehicle Dynamics and Powertrain Component	22
2.1. Battery Electric Vehicle	22
2.2. Electrochemical Sources- <i>Battery</i>	Error! Bookmark not defined.
2.5.1. Electrochemical cells.....	23
2.5.2. Electrical Equivalent Circuit	24
2.5.3. Practical Cell Measures	25
2.5.4. Classification of batteries:.....	27
2.3. DC-AC/DC-DC Converter	29
2.4. Permanent Magnet Synchronous Machine (PMSM)	29
2.3.1. Equivalent electric circuit model.....	30
2.5. Traction Motor Characteristics	35
2.6. Tractive Effort and Transmission Requirement	36
2.7. Vehicle dynamics.....	38
2.7.1. Aerodynamic drag.....	39
2.7.2. Rolling resistance	40
2.7.3. Grading force	41
2.7.4. Wheel force.....	42
2.7.5. Wheel power and energy.....	43
2.8. Vehicle performance.....	43
Chapter 3: Electric Motor Design-optimization Overview.....	44
3.1. Overview	44
3.2. Traditional method for electric machine design.....	44
3.3. Optimization of Electric Motor Design.....	46
3.3.1 Genetic Algorithm	47
Chapter 4: Permanent magnet Synchronous Motor Optimization	49
4.1. Definition of the base design	49

4.2.	Design methodology	53
4.3.	Sensitivity analysis	56
Chapter 5:	Optimization results.....	62
5.1.	Flat-shape.....	62
5.2.	V-shape	63
5.3.	Delta-shape	64
5.4.	Comparison	66
Chapter 6:	Vehicle analysis results- optimal gear ratio	68
Chapter 7	Conclusion of the thesis	76
Bibliography		79

List of figures

Figure 1 Electric Motor Configuration	13
Figure 2 Diagram of general electric machine design.....	15
Figure 3 Motor-CAD view.....	15
Figure 4 Toyota Motor Corporation.....	17
Figure 5 Toyota Motor Europe Center.....	18
Figure 6 Subsidiaries and related company	19
Figure 7 BEV drive system.....	23
Figure 8 Simple Electrolytic cell [7]	24
Figure 9 Equivalent circuit of ideal cell	24
Figure 10 Practical equivalent diagram of cell.....	25
Figure 11 General discharge characteristics of a Lead acid cell.....	25
Figure 12 Discharge times at different at different C-Rates	27
Figure 13 Construction of Lead Acid battery	28
Figure 14 Construction of Nickel Based battery	28
Figure 15 Construction of Li-ion battery	29
Figure 16 Permanent Magnet synchronous motor	31
Figure 17 Equivalent Circuit of an interior PMSM	33
Figure 18 The stator flux linkage in the dq reference frame	34
Figure 19 Typical variable-speed electric motor characteristics	35
Figure 20 Speed–torque profile of a 60 kW electric motor with x 2, 4, and 6.....	36
Figure 21 Tractive effort vs. vehicle speed with a traction motor of x 2 and three-gear transmission	37
Figure 22 Tractive effort vs. vehicle speed with a traction motor of x 4 and two-gear transmission..	37
Figure 23 Tractive effort vs. vehicle speed with a traction motor of x 6 and single-gear transmission	38
Figure 24 Illustration of the iterative design process in the traditional machine design	44
Figure 25 Standard search procedure of genetic algorithm	48
Figure 26 Motor Cad representation of NISS1 motor active parts.....	50
Figure 27 Winding configuration	51
Figure 28 Wire configuration	51
Figure 29 Magnetic characteristics of (N35) NdFeB grade	53
Figure 30 Cross section of “Delta shape”- “V shape”- “FLat shape”.....	53
Figure 31 Design and optimization process	54
Figure 32 Rotor parameters evaluation.....	56
Figure 33 Rotor parameters.....	56
Figure 34 Effect of magnet size on shaft torque.....	57
Figure 35 Effect of magnet size on shaft torque.....	57
Figure 36 Magnet position	58
Figure 37 Effect of the magnet position on torque ripple	58
Figure 38 Effect of the magnet position on shaft torque and power	58
Figure 39 Magnet V-angle.....	59
Figure 40 Effect of magnet V-angle on shaft torque and torque ripple	59
Figure 41 Stator parameters evaluation	60
Figure 42 Stator parameters	60
Figure 43 Flat-shape Optimized design.....	62
Figure 44 Flat-shape Base design.....	62

Figure 45 Maximum torque and power versus speed profiles of the optimized flat-shape design.....	62
Figure 46 Flat-shape Efficiency	63
Figure 47 V-shape Base design	63
Figure 48 V-shape Optimized design	63
Figure 49 Maximum torque and power versus speed profiles of the optimized V-shape design.....	64
Figure 50 V-shape Efficiency	64
Figure 51 Delta-shape Optimized design.....	64
Figure 52 Delta-shape Base design	64
Figure 53 Maximum torque and power versus speed profiles of the optimized Delta-shape design .	65
Figure 54 Delta-shape Efficiency.....	65
Figure 55 Optimum desing.....	66
Figure 56 Maximum power versus speed profiles of the optimized design.....	66
Figure 57 Maximum torque versus speed profiles of the optimized design	67
Figure 58 Delta-shape Efficiency.....	70
Figure 59	72
Figure 60 Flat-shape Efficiency	72
Figure 61 V-shape Efficiency	73
Figure 62 Delta-shape Efficiency.....	74
Figure 63 Optimized design	75
Figure 64 Evolution of PMSM	77

Chapter 1: Introduction and objective of research

1.1. Introduction

This thesis is conducted in cooperation with DENERG, Department of Energy of Polytechnic of Torino, Toyota Motor Europe, Belgium and Motor Design Limited, UK .

It is estimated that traction machines will see a 17.4% annual growth rate from 2013 to 2023, and the number of electric machines for electrified vehicles will rise from 44.6 million in 2013 to 147.7 million in 2023. [1]

With the advanced power electronics and modern controls, AC machines have replaced DC machines and dominated the traction machine market. Both asynchronous and synchronous AC machines are utilized in commercially available electrified vehicles. [1]

Induction machines are the most mature technology and have well-established manufacturing techniques as they have been developed for many decades. Induction machine technology also offers relatively lower cost and easier controllability. However, the conductors on the rotor increases the rotor copper losses and, hence, the cooling requirement. This leads to a lower operating efficiency in general, when compared with permanent magnet synchronous machines (PMSM).

On the other hand, using rare-earth permanent magnets enhances the magnetic flux density in the air gap and increases the power- and torque-density of permanent magnet synchronous machines. Therefore, the majority of automotive manufacturers choose permanent magnet synchronous machines as the traction motor in their vehicles [1].

Table 1.1 summarises the advantages and disadvantages of each type of motor. Compared to with the ideal characteristics required of an electric machine for traction application, the PMSM is the type of motor that offers the best efficiency and high-power density, making it the best choice to drive modern electric vehicles.

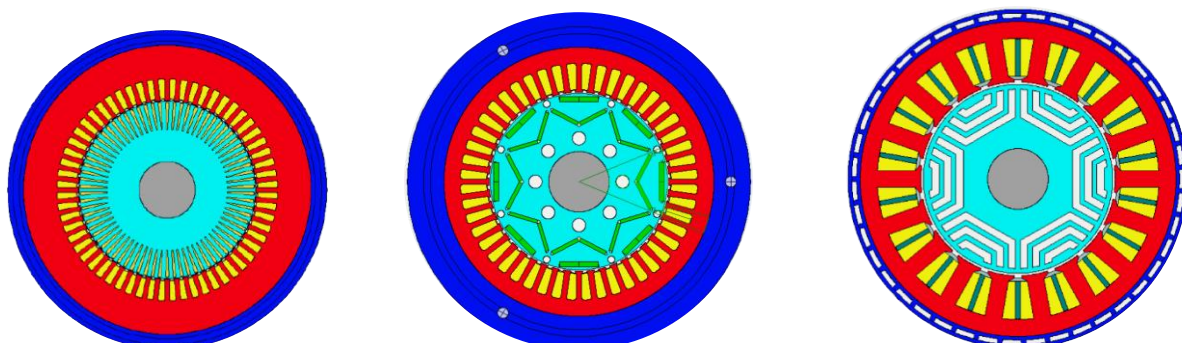


Figure 1 Electric Motor Configuration

Motor Type	Advantages	Disadvantages
PM_SM	<ul style="list-style-type: none"> • High power density • High efficiency 	<ul style="list-style-type: none"> • Limited speed range • High cost • High stator core losses at high speed
Induction Motor (IM)	<ul style="list-style-type: none"> • High speed range • High reliability • Low cost • Rugged in hostile environment 	<ul style="list-style-type: none"> • Low efficiency • Thermal problem at high speed
Switched reluctance motor (SRM)	<ul style="list-style-type: none"> • Desirable torque speed characteristic • High reliability • Low cost • Rigidity in hostile environment 	<ul style="list-style-type: none"> • High torque ripple and noise • Low Power density • Low efficiency

Table 1.1 Advantages and disadvantages of different types of motors[1, 2, 3].

Generally, to accomplish an electric machine design based on optimisation, the designer needs essentially two tools: first, an accurate analytical model to design the electric machine; and second, an efficient optimisation algorithm/software as shown in Figure 1.1 [4]. While the design based on analytical modelling takes its input variables from the optimisation to calculate the relationships between the electromagnetic aspects of the machine, the optimisation studies all the possible input combinations and allows the designer to find a compromise between material properties, machine dimensions, the cost of production and assembly processes that satisfies the design specifications. Therefore, the proposed research is stimulated to design both an accurate analytical design and efficient optimisation.

Motor-CAD is the software used to build the analytical model , it has a specific tool called Motor-opt that has been used for the optimization.

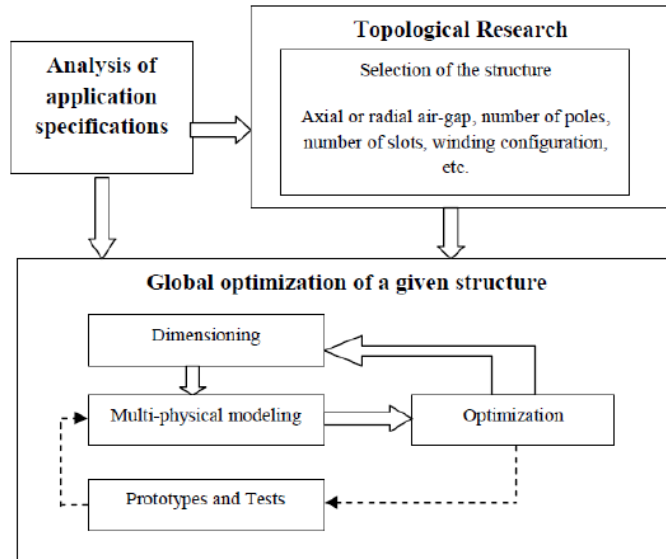
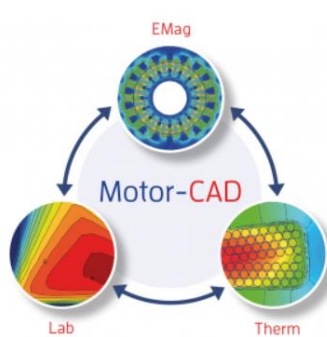


Figure 2 Diagram of general electric machine design

1.2. About Motor-CAD

Motor-CAD is a software package dedicated to the electromagnetic performance of motors and generators and the optimisation of their cooling. Developed in 1998, Motor-CAD is used by major motor manufacturers and universities worldwide.

Motor-CAD provides the ability to quickly and easily perform electromagnetic and thermal performance tests on electric machine designs, using an integrated systems of software packages: EMag, Therm and Lab . Accurate electromagnetic and thermal calculations can be done in minutes. The results are presented in an easy to understand format and allows design decisions to be taken efficiently.



EMag: Offers a fast 2D finite element module for accurate electromagnetic and electrical performance predictions.

Therm: Combines a lumped circuit and finite element thermal calculation for optimising the cooling system of a machine.

Lab: Provides efficiency mapping and duty cycle / drive cycle transient outputs within minutes.

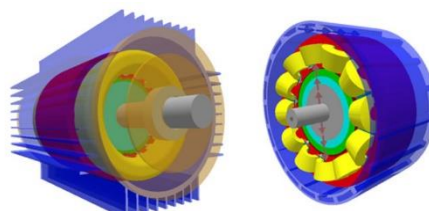


Figure 3 Motor-CAD view

1.3. Motivation and research objectives

This thesis focuses on the design and comparison study of advantages/dis-advantages of the three major Internal Permanent Magnet Synchronous Motor (IPMSM) rotor topologies: the V-shape, the Delta-shape and the Flat-shape.

Using multi-physics simulation (Electro, Thermal) in a C-segment vehicle with fixed performance/packaging requirement.

The design of the electric motor for traction applications encompasses strict requirements and objectives in the machine's size, weight, power density, efficiency and cost, all conflicting with each other. Furthermore, the design of electric machines is a comprehensive mission based on multi-physics electromagnetic, mechanical and thermal models. However, with recent improvements in power electronics, materials and applications, the old, conventional method used to design electric machines has become outdated. Consequently, extensive effort has been devoted to optimising electric machines with respect to different objectives, such as efficiency, power density, cost, and reliability.

Based on specification of a benchmark machine, this thesis describes the design and development of high power density three-phase brushless permanent magnet motors optimized through Genetic Algorithm. The generated new optimal parameters will be used to evaluate the dimensions, electromagnetic and thermal parameters of the new optimised machine, which will be verified by FEA. Then, the performance indices of the resulted machine will be compared with their corresponding values in the benchmark design.

1.4. Toyota Motor Europe

Toyota is one of the world's largest automobile manufacturers and a leading global corporation.

Founded in 1937 by Kiichiro Toyoda to separate the automotive branch from "Toyota Industries", the company is now a multinational corporation headquartered in Japan (Toyota Motor Corporation). In order to improve its establishment in overseas market, Toyota has developed regional headquarters in charge of specific research and development, production and sales related to their location.

Toyota Motor Corporation (TMC) is an automotive manufacturer headquartered in Japan. Formerly integral part of Toyota Industries, this corporation has been created in 1937 to manufacture cars. Nowadays, more than 340 000 people are working for it in more than 160 countries. By producing 10 million vehicles per year, TMC is the second automobile manufacturer and the fourteen-largest company in the planet by revenue. In order to be competitive around the world, TMC have set up local center in each continent (Fig.3): These divisions are necessary to be sure to meet the local market expectations, which can be really different between each continent.

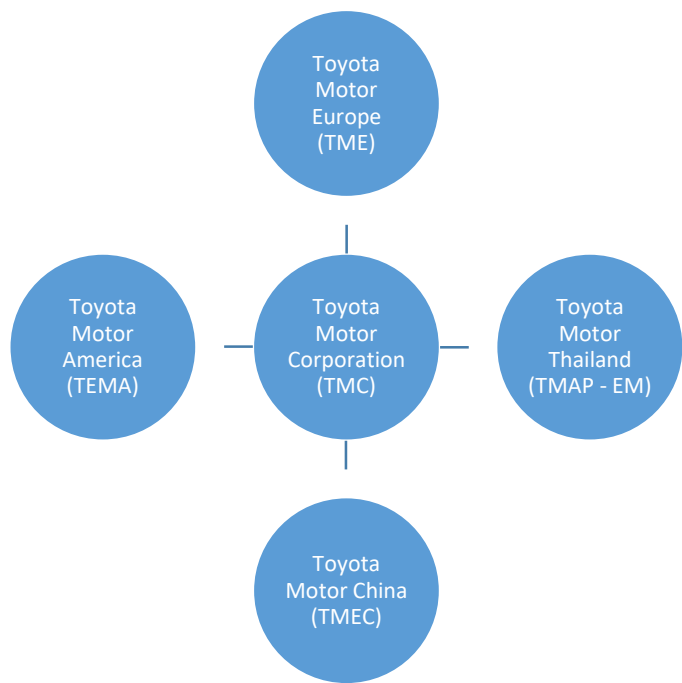


Figure 4 Toyota Motor Corporation

1.4.1. Toyota Motor Europe

Toyota entered the European market in the early 1960s. Since then has been invested more than eight billion Euros in the continent, keeping pace with European vehicle tastes and requirements. Today, 80,000 employees work for Toyota through more than 30 marketing and sales companies in 48 countries and 9 manufacturing plants.



Figure 5 Toyota Motor Europe Center

TME is divided into two sites: the head office is located in Evere near Brussels, that houses key activities for Toyota and Lexus in Europe (HR, after-sales, marketing and top management) and the research and development centre located in Zaventem.

Toyota Technical Centre (R&D) in Europe is responsible for the development and production of attractive, superior quality cars matching European market requirements. As it can be seen on the organization chart below, it works in close collaboration with the different European production plants.

Toyota began selling car in Europe in 1963. Eight billions have been invested to stay competitive regarding the several historical European automotive manufacturers. Nowadays, 80 000 employees work for Toyota Motor Europe through more than 30 marketing and sales companies in 28 countries and 9 manufacturing plants.

The automotive brand established a Head Office in Brussels, where key decisions are taken in the following fields: human resources, after-sales, marketing, top management; and a Technical Centre where the research & development work is carried out.

More specifically, the Technical Centre develops vehicle in agreement with European taste. To be sure to achieve this task, it is divided in several departments, which are specialized in an area to be at the cutting edge of technology: powertrain, vehicle performance engineering, body design, electronics, material, European projects, chassis design and styling.

Toyota Motor Europe (TME) coordinates the European activities of the Toyota group. Within TME, the technical centre is the location for the research & development (600 people), purchasing and production engineering functions. From there Toyota ensures its cars match European customer's high demands.

TME is divided into two sites: the head office which is located in Evere near Brussels, and houses key activities for Toyota and Lexus in Europe (HR, after-sales, marketing and top management). And the research and development centre located in Zaventem (Figure 5).

Toyota Technical Centre (TTC) is responsible for the development and production of attractive, superior quality cars matching European market requirements. As it can be seen on the organization chart below (Figure 5), it works in close collaboration with the different European production plants.

1.4.2. Subsidiaries and related company

Toyota brand includes Scion, for the coupe models sold by Toyota in North America, and Lexus, the luxury division of TMC sold worldwide. TMC also owns stakes in Daihatsu (51.2%), Fuji Heavy Industries (Subaru) (16.66%), Isuzu Motor Ltd. (5.9%) and DENSO (24.74%). All these subsidiaries and stakes allow TMC to be a major player in the global automotive market.

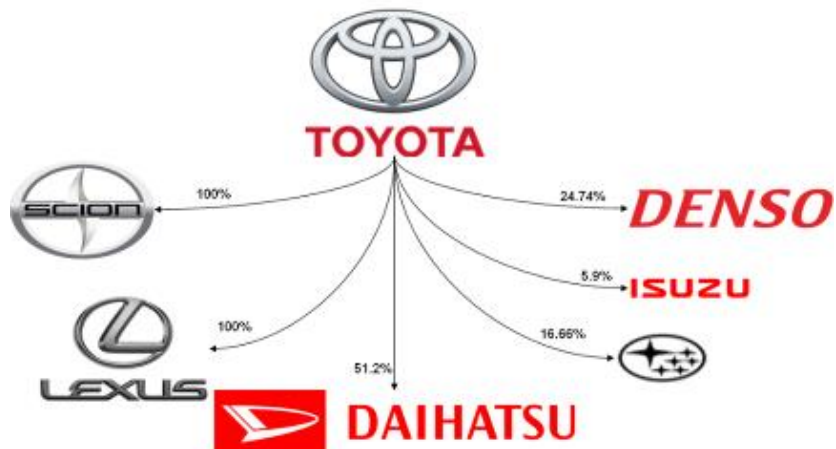
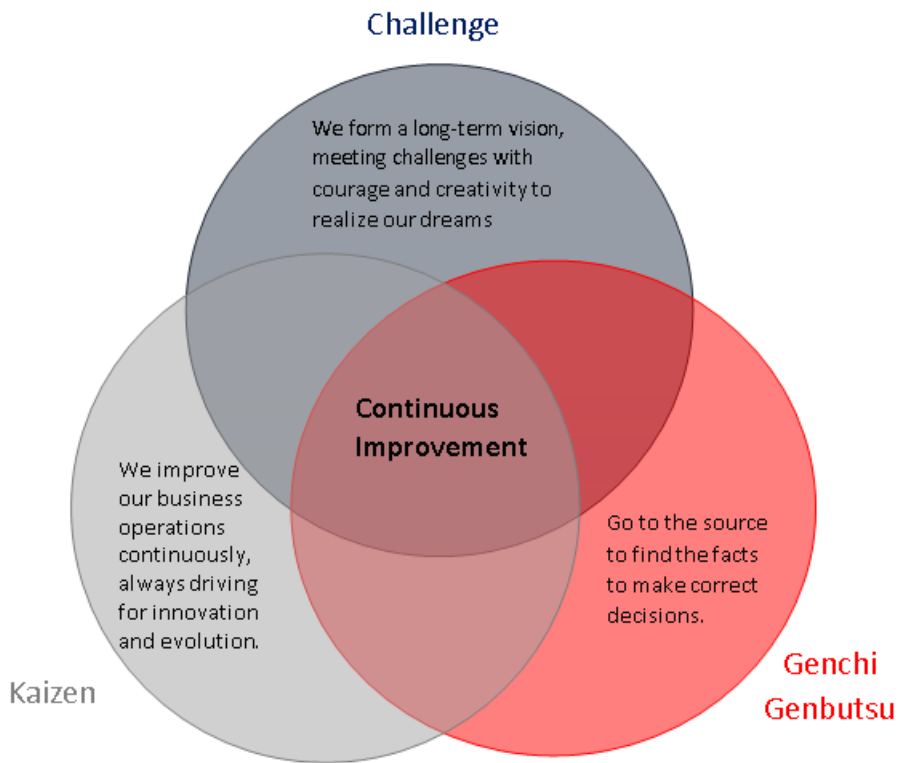


Figure 6 Subsidiaries and related company

1.4.3. The Toyota Way

The Toyota Way is a set of essential principles and behaviors that underlie the Toyota Motor Corporation's managerial approach and production system. Toyota first summed up its philosophy, values and manufacturing ideals in 2001, calling it "The Toyota Way 2001." It consists in two key principles: continuous improvement, and respect for people



1.4.4. Hybrid technology development

Precursor, Toyota was the first OEM (Original Equipment Manufacturer) to make a mass production of hybrid vehicle: the Prius (1997). On the short-term Toyota engagement towards sustainable development comes by increasing the performance and availability of hybrid (petrol/electric) vehicles, and continually making petrol engines more fuel efficient and diesel engines cleaner for today's cars. On a longer term it comes by developing alternative fuels, such as hydrogen and bio-fuels, and more efficient battery-powered electric systems. In 2012 Toyota announced its plans to start retail sales of a hydrogen fuel-cell in USA in 2015. Toyota expects to become a leader in this technology.

Toyota's ultimate objective is the eco-car: a vehicle that produces zero emissions throughout its entire lifecycle.

As an example, all Toyota vehicles – including hybrid parts and batteries – are manufactured and dismantled at the end of their life in ways that maximize energy efficiency and minimize waste. 2020 target is to have 85% of the vehicle weight reused or recycled and 10% recovered as energy, leaving the remaining 5% for disposal.

Chapter 2: Battery Electric vehicle Dynamics and Powertrain Component

2.1. Battery Electric Vehicle

Electric vehicles are by many seen as the cars of the future as they are high efficient, produces no local pollution, are silent, and can be used for power regulation by the grid operator. However, electric vehicles still have critical issues which need to be solved. The three main challenges are limited driving range, long charging time, and high cost.

The powertrain of a Battery Electric Vehicle (BEV) consists of an electric drive system with a battery serving as an energy buffer. Usually there is only one electric machine, typically of three phase AC type, connected to the wheel shaft via a gearbox and a differential. However some applications may utilize several electric machines, e.g. hub wheel motors, but in this specific project it has been considered one EM. The energy is stored chemically in a battery, which is electrically connected to the machine via a DC/AC power electronic converter accompanied by a control system. The control system controls the frequency and magnitude of the three phase voltage that is applied to the electric machine, and these are depending on the driver's present request, which is communicated via the acceleration and/or brake pedal.

In vehicle applications, it is usually desirable to keep the physical volume of the electric machine down. This can be done by designing it for higher speed levels. A reasonable compromise is a maximum speed between 10.000 to 12.000 rpm [1], since it serves as a good compromise between volume and performance.

Still, during normal on road driving the speed range of a vehicle may vary between zero to about 150 km/h or even higher at times. This means that the wheels will spin up to around 1200 rpm or higher. Therefore a reduction gear ratio towards the wheels, is inherently needed.

Additionally, in order to give the left and right traction wheels a chance to spin at slightly different speeds during turning, there is also a need for a differential to be connected between the wheels. Sometimes the differential also includes a final gear ratio. A typical BEV drive system, which is also the type of system studied in this theses, is depicted in Figure 4 .

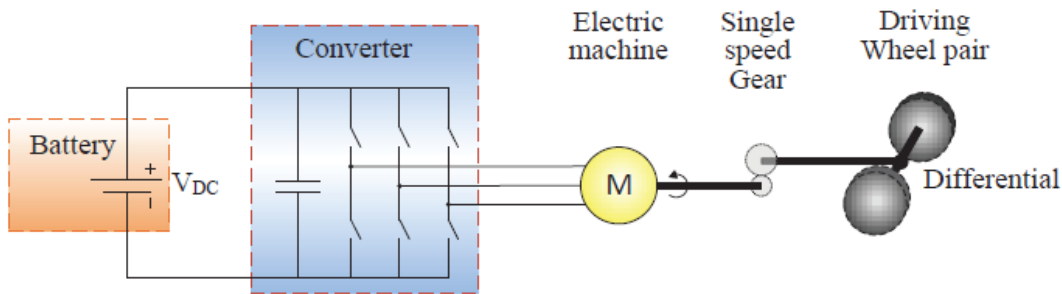


Figure 7 BEV drive system

2.2. Electric Battery

Also known as electric batteries in general, are made by connecting individual cells in order to get a specific standard voltage at their terminals. Batteries are energy devices converting chemical energy to electrical energy, hence the name Electrochemical device. Batteries nowadays play an important role as an energy producing source as well as energy storage devices.

Batteries are primarily made up of individual cells by a suitable connection, therefore we will now focus on the cells to have further understanding of batteries.

2.5.1. Electrochemical cells

Electrochemical cells are primarily a separation of electrodes, one is positive and another negative, filled with electrolyte (must be ionically conductive and electrically insulating) and separated by separator. The voltage produced by a cell is governed by chemical reaction going inside the cell in between the electrodes, facilitated by the electrolyte. We can consider electrochemical cells in two types, *Electrolytic cells* and *Galvanic cells*. When chemical energy is converted to electrical energy, then it is known as *galvanic cell* and when electrical is converted to chemical energy then it is called as *electrolytic cell*. Hence, we can say that electrochemical cell works in two different modes, while charging it is *electrolytic cell* and while discharging it becomes *galvanic cell*. (10).

During discharging, electrolytic cell operation, oxidation or release of electron occurs at the anode while charging, absorption of electrons occurs on the anode. On the cathode the opposite occurs, reduction or electron while discharging and while charging oxidation or reduction of electro occurs. As it can lead to confusion that both electrodes are undergoing both anodic and cathodic reaction depending on if cell is in under charging mode or discharging mode. Thus, in order to avoid any confusion, negative electrode is referred as *anode*, and positive electrode is termed as *cathode*, as widely accepted. Considering electrolytic cell, electrons are absorbed at the negative electrode and

released at positive electrode. It is then apparent that the reduction going on on the negative electrode and oxidation going on on the positive electrode, due to result of chemical reaction interaction at both electrodes. These chemical reactions are known as half reactions, when combined leads to the total cell reaction, i.e. *redox* reaction, by virtue of which our cell works.

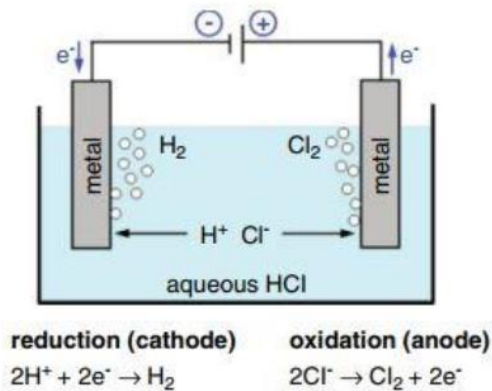


Figure 8 Simple Electrolytic cell [7]

The figure above demonstrates decomposition of dilute HCl into Hydrogen and Oxygen. We can also see that reduction is going on cathode and oxidation is going on anode. The reactions at anode and cathode are the reactions referred as half reactions, and adding both equations we get cell equation which in this case would be,

$$2HCl = Cl_2 + H_2 \quad (1)$$

2.5.2. Electrical Equivalent Circuit

Out of different methods to model electrochemical cells, electrical equivalent modelling is the most convenient. It is relatively simple, compared to other models such as electrochemical model and also easy to understand.

Equivalent circuit diagram :

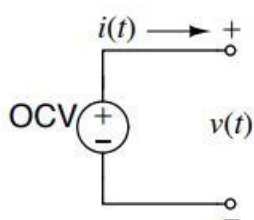


Figure 9 Equivalent circuit of ideal cell

Properties of an ideal cell are:

- OCV, open circuit voltage is not a function of current
- Voltage is not a function of past usage
- Voltage is constant throughout its life time. [11]

As we know, that ideal cell does not exist in the real world. Every cell will have an internal resistance, which can explain the battery's rise in temperature when loaded [12].

Moreover, battery model also consists of a parallel connected resistance and capacitance in addition to the internal resistance to show the transient nature of battery. In order to improve accuracy of the practical model, we can add more parallel connection of resistance and capacitance. But in general modelling, accuracy obtained by single parallel branch is sufficient. [13] [11]

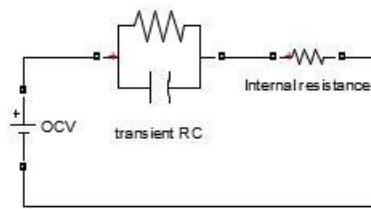


Figure 10 Practical equivalent diagram of cell

With the introduction of the electric cell, we will move to the technical parameters and characteristics of the cell which play a vital role in selecting right battery source of specific application.

2.5.3. Practical Cell Measurement

As we learnt about cells, both ideal and practical, we can now further study the cell under load. The discharge curve of lead acid cell is shown below,

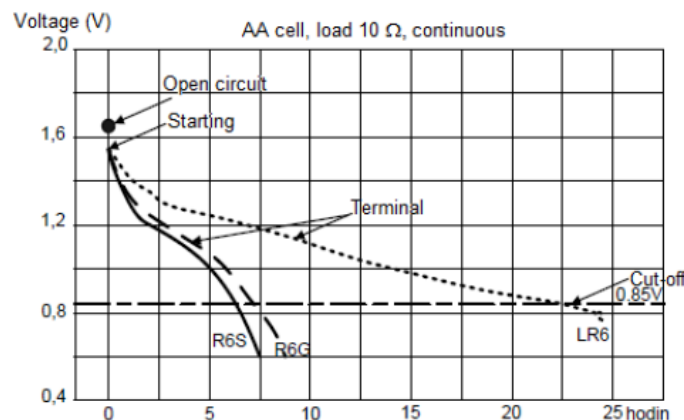


Figure 11 General discharge characteristics of a Lead acid cell

The cell properties which are of our interest are as follows:

1. Terminal Cell Voltage: The voltage measured across the terminals of cell is known as cell voltage when the cell is applied to any application with certain load. Thus, open circuit voltage is higher than the nominal cell voltage [15]. It is because, during discharge, as the chemical energy is transformed into electrical energy, the open circuit voltage also drops to the nominal voltage due to the losses in cell. Polarisation or overpotential occurs when a load current is passing through the cell. The dominant cause of loss in the cell is due to internal resistance resulting into ohmic losses. In addition to this, the internal resistance causes voltage drop, when load current is passed through during discharge, which is referred as ohmic polarisation, which is directly proportional to discharge current applied. [15]
2. Cut-off voltage: Voltage level at the terminals of the battery at which battery is said to be empty or zero state of charge. And prohibited to use in the application in order to prevent permanent loss in capacity of the battery. [15]
3. State of Charge (SOC): It is a percentage of instantaneous battery capacity left out of total battery capacity. SOC can be calculated by integrating battery current over a period of time. [14][15]
4. Depth of Discharge (DOD): the percentage of battery capacity discharged in the terms of total capacity is known as depth of discharge. Generally, DOD can be related to SOC as follows; $DOD=1-SOC$; (when expressed in fraction) [11]
5. Capacity: Also known as coulometric capacity, absolute Ah (*ampere hours*) available at a certain C-rate (defined later), when battery goes from 100% SOC (*state of charge*) to 0% SOC. [16]
6. Charge and discharge rates: The charging and discharging of the battery is termed as C-rate. The discharge and charge rate depend upon the electrochemical reaction and movement of ion in the electrolyte of cell. Also, it depends upon internal resistance of cell. As we change our discharge and charge rate, other parameters such as *State of Charge (SOC)*, *lifetime period*, *life cycle*, etc will change. Charge and discharge rates are governed by the *C-Rate*. The *capacity* of the battery is rated as 1C, which implies that fully charged battery of 1Ah rating is going to deliver 1 Ampere for 1 Hour. Following the table below, meaning of C-rate can be comfortably understood. [16][17]

<u>C-Rate</u>	<u>Time</u>
5C	12 mins
2C	30 mins
1C	1 hour
0.5C or C/2	2 hours
0.1C or C/10	5 hours

Figure 12 Discharge times at different C-Rates

7. Battery lifetime: the time after which the battery is unable to meet 80% of rated capacity at full charge, after a significant number of charge and discharge cycles. Conditions like rate of discharge, depth of discharge, temperature, humidity, etc. are responsible for determining battery operating life. [14]
8. Specific Energy: Specific energy depends upon the battery chemistry and packaging.
9. Specific Power: Specific power also depends upon chemistry and packaging. It is defined by the ratio of available maximum power over the mass. Specific power has a unit of watt/kg. It is vital to know about the battery capability to deliver power to meet high power application, such as start, acceleration and climbing a slope [16].
10. Energy Density: The battery energy per unit volume is known as energy density. It is required to determine the range of vehicle. Its unit is watt-hour/L. [16]
11. Power Density: It is the maximum available power per volume of battery. Its unit is watt/kg. [16]

2.5.4. Classification of batteries:

Based upon electrode material, with respect to EV application, there are majorly 5 types of accumulators available.

- a) Lead Acid Accumulator: Being in existence from approximatively the last 140 years, it is one of the most widely used technologies in automotive technology in order to provide electric power to the starter motors. [14][15]

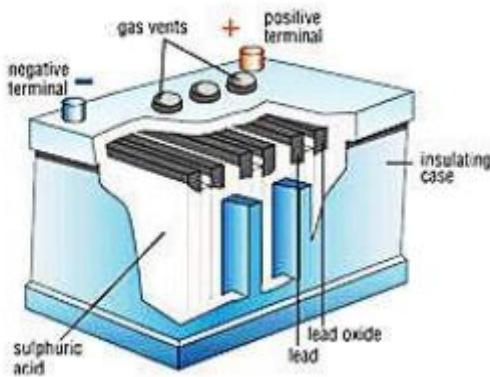


Figure 13 Construction of Lead Acid battery

b) Nickel Based Accumulators:

There are three well known *Ni based* accumulators, namely Nickel Zinc (NiZn), Nickel Cadmium (NiCd) and Ni metal hydride (NiMh) accumulator. In general, Ni based accumulators have positive electrode as Ni, and negative electrode depends upon type of accumulator being considered, e.g. for NiCd battery, Positive electrode will be made out of *Nickel(Ni)* and negative electrode will be made of *Cadmium (Cd)*. *NiZn* batteries have higher *nominal voltage* as compared to *NiCd* and *NiMH* variant of the nickel-based battery. (14)

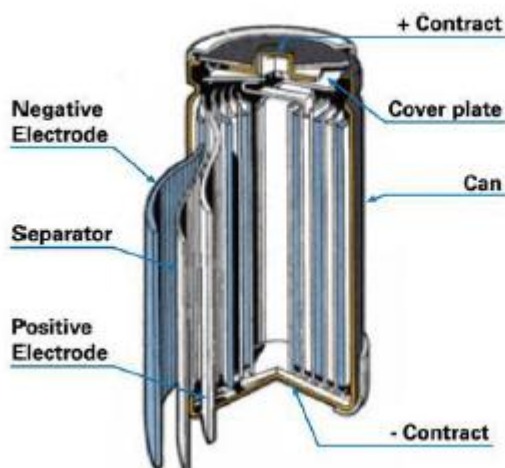


Figure 14 Construction of Nickel Based battery

c) Lithium –Ion battery:

Lithium being the lightest metal present (0.54 kg/dm³) with low electrochemical potential of about $-3.04\text{ V vsH}_2\text{H}^+$, makes it the most reactive among metals. In addition, lithium has a very low radius of about 0.76 angstroms. Being small in radius, lithium can be easily accommodated into different shape.

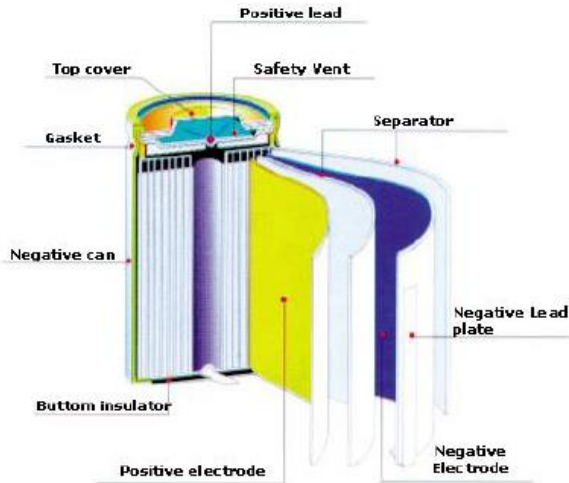


Figure 15 Construction of Li-ion battery

2.3. DC-AC/DC-DC Converter

A DC-AC converter typically utilizes power electronic switching devices in order to convert between the battery DC voltage and the three phase AC voltage which is demanded by the electric machine. In automotive application each switch normally consist of one or a few paralleled IGBT chips in parallel with one or a few diode chips, depending on current rating.

2.4. Permanent Magnet Synchronous Machine (PMSM)

The use of permanent magnets (PMs) in construction of electrical machines brings the following benefits:

- No electrical energy is absorbed by the field excitation system and thus there are no excitation losses, which means substantial increase in efficiency,
- Higher power density and/or torque density than when using electromagnetic excitation, such as with induction motors or wound-field synchronous motors.
- Better dynamic performance than motors with electromagnetic excitation (higher magnetic flux density in the air gap),
- Simplification of construction and maintenance,
- Reduction of prices for some types of machines.

The first PM excitation systems were applied to electrical machines as early as the 19th century, e.g., J. Henry (1831), H. Pixii (1832), W. Ritchie (1833), F. Watkins (1835), T. Davenport (1837), M.H. Jacobi (1839).

Of course, the use of poor quality hard magnetic materials (steel or tungsten steel) soon discouraged their use in favor of electromagnetic excitation systems. The invention of Alnico in 1932 revived PM excitation systems; however, its application was limited to small and fractional commutator machines. At the present time most PM D.C. commutator motors with slotted rotors use ferrite magnets.

Cage induction motors have been the most popular electric motors in the 20th century. Recently, owing to the dynamic progress made in the field of power electronics and control technology, their application to electrical drives has increased. Their rated output power ranges from 70 W to 500 kW, with 75% of them running at 1500 rpm. The main advantages of cage induction motors are their simple construction, simple maintenance, no commutator or slip rings, low price and moderate reliability. The disadvantages are their small air gap, the possibility of cracking the rotor bars due to hot spots at plugging and reversal, and lower efficiency and power factor than synchronous motors.

The use of PM brushless motors has become a more attractive option than induction motors. Rare earth PMs can not only improve the motor's steady state performance but also the power density (output power-to-mass ratio), dynamic performance, and quality. The prices of rare earth magnets are also dropping, which is making these motors more popular. The improvements made in the field of semiconductor drives have meant that the control of brushless motors has become easier and cost effective, with the possibility of operating the motor over a large range of speeds while still maintaining good efficiency.

2.3.1. Equivalent electric circuit model

The d- and q-coordinate based equivalent circuit model is used for the modelling of PMSMs. Fig. 15 illustrates a conceptual cross-sectional view of a 3-phase, 2-pole interior PMSM along with two reference frames. To show the inductance difference ($L_q > L_d$), rotor is drawn with saliency.

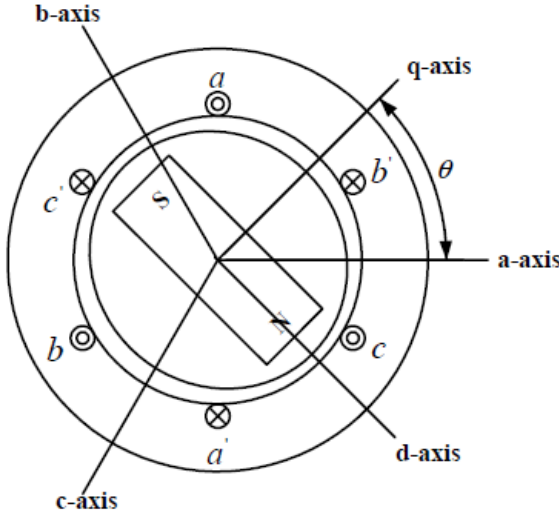


Figure 16 Permanent Magnet synchronous motor

The electrical dynamic equation in terms of phase variables can be written as:

$$V_a = R_s I_a + \frac{d\lambda_a}{dt} \quad (2)$$

$$V_b = R_s I_b + \frac{d\lambda_b}{dt} \quad (3)$$

$$V_c = R_s I_c + \frac{d\lambda_c}{dt} \quad (4)$$

Where (V_a, V_b, V_c) , (I_a, I_b, I_c) and R_s refer to phase voltage, current and resistance respectively. The phase flux linkage $(\lambda_a, \lambda_b, \lambda_c)$ equations are:

$$\lambda_a = L_{aa} I_a + L_{ab} I_b + L_{ac} I_c + \lambda_{ma} \quad (5)$$

$$\lambda_b = L_{ab} I_a + L_{bb} I_b + L_{bc} I_c + \lambda_{mb} \quad (6)$$

$$\lambda_c = L_{ac} I_a + L_{bc} I_b + L_{cc} I_c + \lambda_{mc} \quad (7)$$

where $(\lambda_a, \lambda_b, \lambda_c)$ refer to the component of phase flux linkage provided by permanent magnets. In these equations, inductances are functions of the angle θ .

Since stator self-inductances are maximum when the rotor q-axis is aligned with the phase axis, while mutual inductances are maximum when the rotor q-axis is in the midway between two phases. Also, the effects of saliency appeared in stator self and mutual inductances are indicated by the term 2θ . Meanwhile, flux linkage at the stator windings due to the permanent magnet are:

$$\lambda_{ma} = \lambda_m \cos \theta \quad (8)$$

$$\lambda_{mb} = \lambda_m \cos(\theta - \frac{2\pi}{3}) \quad (9)$$

$$\lambda_{mc} = \lambda_m \cos(\theta + \frac{2\pi}{3}) \quad (10)$$

For this model, input power P_{in} can be represented as:

$$P_{in} = \vec{V}_a \vec{I}_a + \vec{V}_b \vec{I}_b + \vec{V}_c \vec{I}_c \quad (11)$$

Let S represent any of the variables (current, voltage, and flux linkage) to be transformed from the a–b–c frame to d–q frame through the Park's transformation:

$$\begin{bmatrix} S_q \\ S_d \\ S_0 \end{bmatrix} = \frac{2}{3} \begin{bmatrix} \cos \theta \cos(\theta - 2\pi/3) & \cos(\theta + 2\pi/3) \\ \sin \theta \sin(\theta - 2\pi/3) & \sin(\theta + 2\pi/3) \\ \frac{1}{2} & \frac{1}{2} \end{bmatrix} \begin{bmatrix} S_a \\ S_b \\ S_c \end{bmatrix} \quad (12)$$

With these transformations the stator voltage equations in d–q frame of PMSM are:

$$v_d = R i_d + \frac{d\lambda_d}{dt} - \omega_s \lambda_q \quad (13)$$

$$v_q = R i_q + \frac{d\lambda_q}{dt} - \omega_s \lambda_d \quad (14)$$

Where

$$\lambda_q = \lambda_{aq} = L_q i_q \quad (15)$$

$$\lambda_d = \lambda_{ad} + \lambda_m = L_d i_d + \lambda_m \quad (16)$$

λ_m is the permanent magnet flux linkage. Fig. XX shows a dynamic equivalent circuit of an interior PMSM in d – q frame.

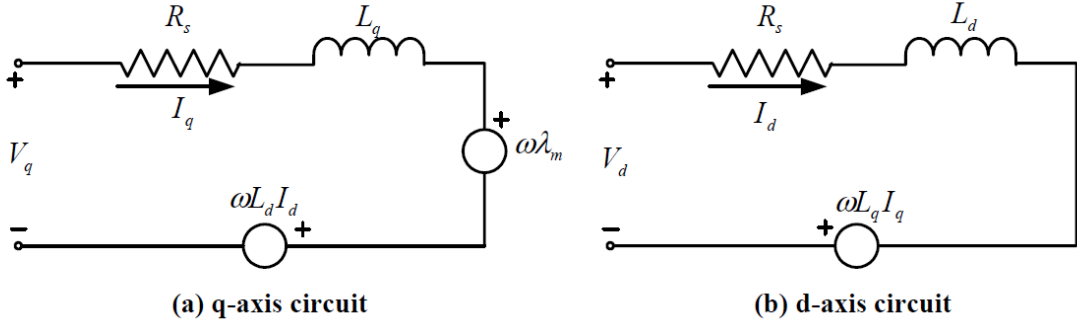


Figure 17 Equivalent Circuit of an interior PMSM

According to the equivalent circuit, the phasor diagram of an interior PMSM can be drawn in Fig. 10. For this model, input power can be derived from (3.2.12) via Park transformation (3.2.11) as:

$$P_{in} = [v_a \ v_b \ v_c] \begin{bmatrix} i_a \\ i_b \\ i_c \end{bmatrix} = \frac{3}{2} [v_q \ v_d] \begin{bmatrix} i_q \\ i_d \end{bmatrix} = \frac{3}{2} (v_q i_q + v_d i_d) \quad (17)$$

Neglecting the zero sequence quantities, the output power can be obtained by replacing Vq and Vd (3.2.12) by the associated speed excited back EMF $\omega_s \lambda_d$ and $-\omega_s \lambda_q$ as:

$$P_o = \frac{3}{2} (-\omega_s \lambda_q i_d + \omega_s \lambda_d i_q) \quad (18)$$

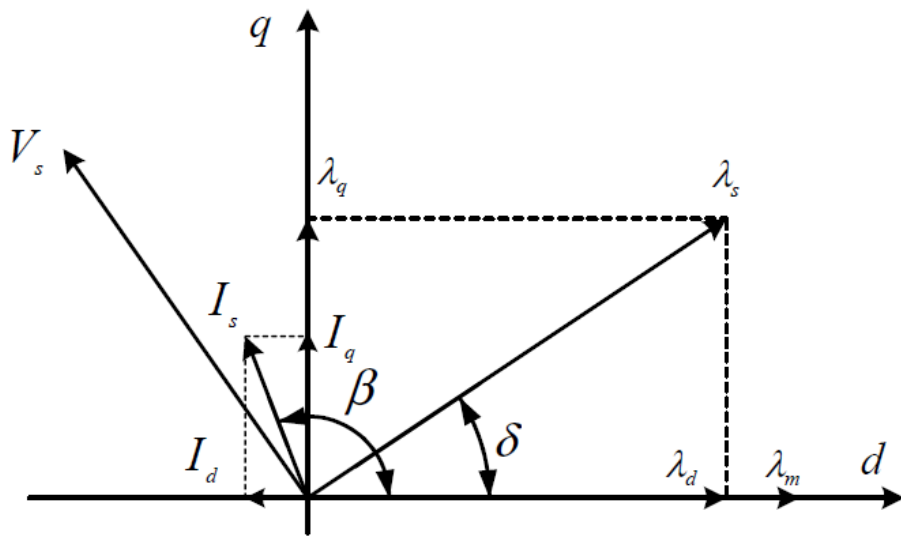


Figure 18 The stator flux linkage in the dq reference frame

The electromagnetic torque, which is power divided by mechanical speed can be represented as:

$$T_e = \frac{3P}{2} \left[\lambda_m i_q + (L_d - L_q) i_q i_d \right] \quad (19)$$

It is apparent from the above equation that the torque is composed of two distinct mechanisms. The first term corresponds to "the magnet excitation torque" or "synchronous torque" occurring between I_q and the permanent magnet, while the second term corresponds to "the reluctance torque" due to the difference in d-axis and q-axis reluctance (or inductance). Thus the torque equation suggests that the interior PMSMs can be interpreted as hybrid combination of the conventional synchronous-reluctance motors and exterior permanent magnet motors.

2.5 Traction Motor Characteristics

Electric motor drives usually have the characteristics shown in Figure 18 . At the low-speed region (less than the base speed as marked in Figure 17), the motor has a constant torque. In the high-speed region (higher than the base speed), the motor has a constant power. This characteristic is usually represented by a speed ratio x , defined as the ratio of its maximum speed to its base speed. In low-speed operations, voltage supply to the motor increases with the increase of the speed through the electronic converter while the flux is kept constant. At the point of base speed, the voltage of the motor reaches the source voltage. After the base speed, the motor voltage is kept constant and the flux is weakened, dropping hyperbolically with increasing speed.

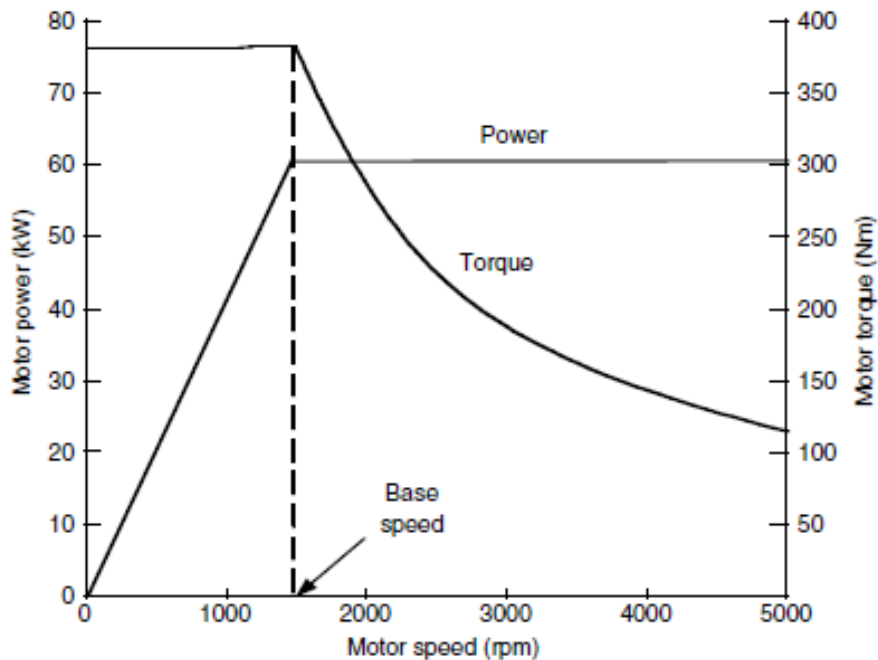


Figure 19 Typical variable-speed electric motor characteristics

Hence, its torque also drops hyperbolically with increasing speed.^{3,4,5} Figure 19 shows the torque–speed profiles of a 60 Kw motor with different speed ratios x ($x=2, 4, \text{ and } 6$). It is clear that with a long constant power region, the maximum torque of the motor can be significantly increased, and hence vehicle acceleration and gradeability performance can be improved and the transmission can be simplified. However, each type of motor inherently has its limited maximum speed ratio. For example, a permanent magnet motor has a limited maximum speed ratio. For example, a permanent magnet motor has a small x , because of the difficulty of field weakening due to the presence of the permanent magnet. Switched reluctance motors and induction motors may achieve higher value.

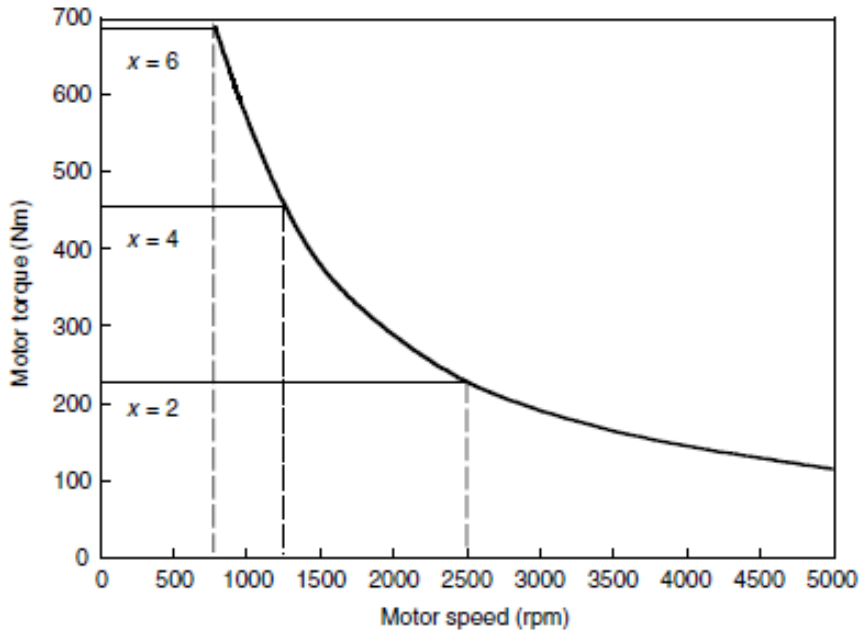


Figure 20 Speed–torque profile of a 60 kW electric motor with $x = 2, 4$, and 6

2.6 Ttractive Effort and Transmission Requirement

The tractive effort developed by a traction motor on driven wheels and the vehicle speed are expressed as:

$$F_t = \frac{T_m i_g i_0 \eta_t}{r_d} \quad (20)$$

And

$$V = \frac{\pi N_m r_d}{i_0 30 i_g} \quad (21)$$

where T_m and N_m are the motor torque output and speed in rpm, respectively, i_g is the gear ratio of transmission, i_0 is the gear ratio of final drive, η_t is the efficiency of the whole driveline from the motor to the driven wheels, and r_d is the radius of the drive wheels. The use of a multigear or single-gear transmission depends mostly on the motor speed–torque characteristics. That is, at a given rated motor power, if the motor has a long constant power region, a single-gear transmission would be sufficient for a high tractive effort at low speeds. Otherwise, a multigear (more than two gears) transmission has to be used. Figure 20 shows the tractive effort of an EV, along with the vehicle speed with a traction motor of $x=2$ and a three-gear transmission. The first gear covers the speed region of a–b–c, the second gear covers d–e–f, and the third gear covers g–f–h. Figure 21 shows the tractive effort with a traction motor of $x=6$ and a two-gear transmission. The first gear covers the speed region

of a–b–c and the second gear d–e–f. Figure 22 shows the tractive effort with a traction motor of x 6 and a single-gear transmission. These three designs have the same tractive effort vs. vehicle speed profiles. Therefore, the vehicles will have the same acceleration and gradeability performance.

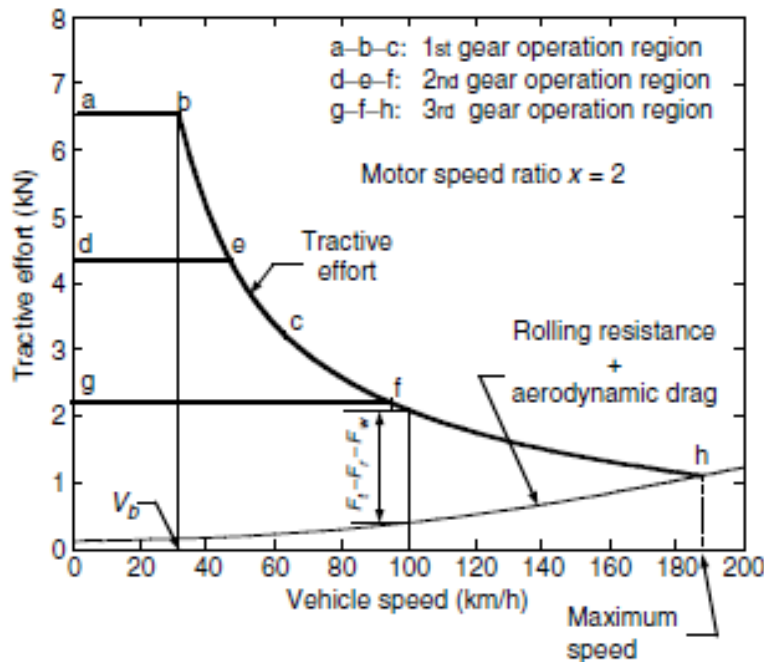


Figure 21 Traction effort vs. vehicle speed with a traction motor of x 2 and three-gear transmission

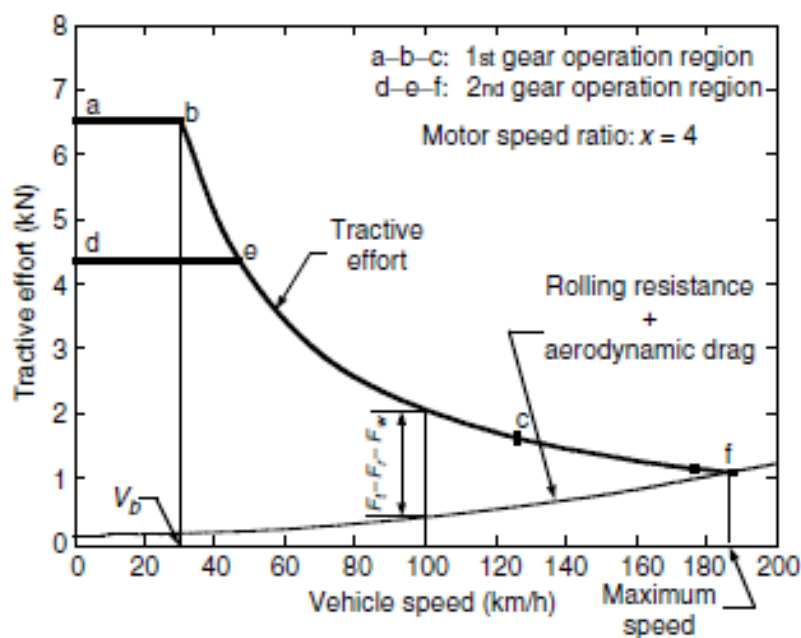


Figure 22 Traction effort vs. vehicle speed with a traction motor of x 4 and two-gear transmission

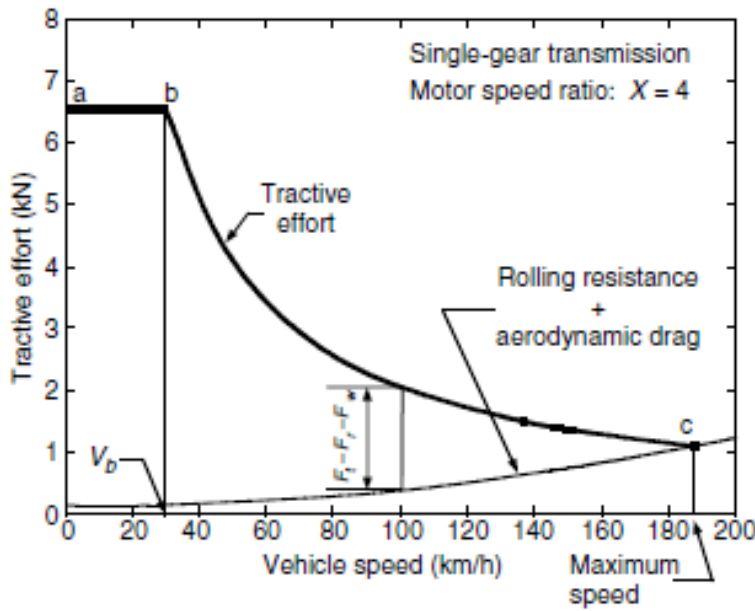


Figure 23 Tractive effort vs. vehicle speed with a traction motor of $x 6$ and single-gear transmission

2.7 Vehicle dynamics

Vehicle dynamics aim to describe how a vehicle moves on a road surface while it is under the influence of forces between the tire and the road, as well as aerodynamics and gravity. During the powertrain design phase, basic knowledge in vehicle dynamics is essential since it reveals what loads and load levels that the powertrain needs to cope with during driving. The understanding of vehicle dynamics is equally important while evaluating the powertrain's impact on the vehicle's performance (usually assessed through simulations), whether it may be time to accelerate, or average energy consumption per driven distance. As with modeling of any object, a rolling vehicle can be modeled with various levels of detail depending on what main phenomena that is targeted to be studied. For the type of dynamical studies in this thesis, where powertrain load levels and energy consumption will be analyzed, it is reasonable to assume that the vehicle body is rigid, hence it can be modeled as a lumped mass at the vehicle's center of gravity.[2] Furthermore, only dynamics in one direction, the longitudinal forward direction, is of interest while under the assumption that vehicle stability is not under any circumstances violated.

According to Newton's second law of mechanics, the dynamical movement of a vehicle in one coordinate axis is entirely determined by the sum of all the forces acting on it in that same axis of direction, as described in the translational form

$$ma = m \frac{d}{dt} v(t) = F_{tractive}(t) - F_{resistive}(t) \quad (22)$$

where m (kg) is the equivalent mass to be accelerated including possible rotating inertias in the powertrain, a (m/s^2) and $\frac{d}{dt}v(t)$ is the time rate of change of vehicle speed $v(t)$ (m/s), i.e. acceleration a (m/s^2), $F_{\text{tractive}}(t)$ (Nm) is the sum of all the tractive forces acting to increase the vehicle speed and $F_{\text{resistive}}(t)$ is the sum of the resistive forces acting to decrease the speed.

The main tractive force is the one exerted from the powertrain via the gear, differential and the wheel shaft to the contact area between the wheels and the road. During downhill driving gravity may also serve as a major tractive force, however during uphill driving it may instead be a large resistive force. Other major resistive forces are aerodynamic drag and rolling resistance, as well as regenerative braking using the electric power train and braking using conventional friction brakes.

IN short, a vehicle will accelerate when the sum of the tractive forces is larger than the sum of the resistive forces, and thus will decelerate when the opposite applies. To keep a constant speed the net resistive force must be exactly matched by the net tractive force.

2.7.1. Aerodynamic drag

The aerodynamic drag that any vehicle unavoidably is exposed to during driving, springs from the flow of air around and through the vehicle which are also often referred to as external and internal flows. Due to the complex shape of automobiles, and to the even more complex nature offluid dynamics, accurate and reliable analytical models of aerodynamical drag are verydifficult to develop, even with advanced CFD softwares at hand. A compromise that isoften used to model the aerodynamical drag force, F_a , is partly empirical, and partlybased on the expression of dynamical pressure, which is showing a strong dependanceon the square of the vehicle speed as

$$F_a = \frac{1}{2}\rho A_f C_D (v_{car} + v_{wind})^2 \quad (23)$$

where ρ (kg/m^3) is the air density, C_D the aerodynamic drag coefficient, A_f (m^2) is the effective cross sectional area of the vehicle, v_{car} (m/s) is the vehicle speed and v_{wind} (m/s) is the component of wind speed moving in the direction of the vehicle [2]. The aerodynamical drag thus increases with head wind speeds. A head wind speed of 10 m/s gives an added drag equal to a vehicle driving 36 km/h in no wind, and one of 25 m/s gives a drag equal to a vehicle speed of 90 km/h. Still, the direction of the wind that hits the vehicle is rather random, and non-head winds increase not only the vehicle's effective cross sectional area, but also the aerodynamic drag coefficient by around 5 to 10% for passenger cars in common wind conditions (slightly more for family sedans and slightly less for sports cars), according to [2].

Air density varies depending on temperature, humidity and pressure, where the later indicates an altitude dependance. For comparative studies, often the density value of $1.225 \text{ (kg/m}^3)$ is used, which represents standardized conditions such as dry air at 15°C at standard atmospheric pressure (1013.25 Pa) i.e. at sea level [2]. For temperatures between -30 to 50°C the density of dry air may be 80 to 110% of the standard air density, while an increase in altitude of about 300 m above sea level leads to a decrease in the dry air density of about 3% relative to the standard air density [3].

The effective cross sectional **area** of the vehicle varies depending on the vehicle size and shape. For auto manufacturers, the value of a certain car model's area can be found through detailed drawings or perhaps wind tunnel tests, yet the resulting value is not always communicated in official vehicle specifications. Therefore external parties are often forced to make rough estimations which relate the area to the product of a vehicle's height and width or track width. Various such estimations can be found in literature; 79 - 84 % in [4], 81 % in [5] and 90 % of the product of track width and height in [6].

The **drag coefficient**, C_D is a dimensionless parameter that represents all the drag effects that are active on the vehicle, i.e. both external and internal. To acquire an accurate estimate it has to be measured. Therefore, automotive manufacturers measure the total drag force, F_d in wind tunnels or coast down tests as well as the cross sectional area, air density and vehicle speed. Then, the drag coefficient can be found.

In comparison to area, this parameter is often made official and communicated in car model specifications. Typically the C_D value is in the range 0.25-0.35 in today's passenger cars [5], yet it may vary between 0.15 for a more streamlined shape up to 0.5 or higher for open convertibles, off-road vehicles or other rough shaped vehicles. Furthermore, the C_d value will change if the airflow around and through the vehicle is altered during driving, for instance an open side window may increase the C_D value by about 5 % [5]. During the last few decades the general trend has been decreasing C_D values on new passenger cars [6], much due to the increased interest in fuel efficiency and emissions. In order not to compromise too much on the design and compartment comfort for the passengers, most work on aerodynamical drag reduction is likely to be focused on the C_D value [6] rather than on the area.

2.7.2. Rolling resistance

Rolling resistance is caused by a number of different phenomena taking place in and around the car tires during rolling. One of the major effects is that the repeated deflection of the tire causes a

hysteresis within the tire material, which gives rise to an internal force resisting the motion [5]. Still, according to [3] rolling resistance depends on more than seven different phenomena, which makes estimation of rolling resistance through analytical modelling very difficult. Therefore, the rolling resistance force, F_r acting on a vehicle in the longitudinal direction, is usually expressed as the effective normal load of the vehicle multiplied by the dimensionless rolling resistance coefficient, f_r as :

$$F_r = Mg f_r \cos \alpha \quad (24)$$

where M (kg) is the vehicle mass, g (m/s^2) is the gravity constant, α (rad) is the road inclination angle. Often the $\cos(\alpha)$ term is neglected since even a large grade such as 10% ($\alpha \approx 0.1$ rad), means that $\cos(\alpha) \approx 0.995$ i.e. an error of less than 0.5% of the rolling resistance force.

Empirical studies show that the f_r value depends on factors such as; tire material and design, but also tire working conditions such as inflation pressure (f_r decrease with increasing pressure), tire temperature (f_r decrease with increasing temperature), road surface (structure, wet or dry) and speed (f_r increase with increasing speed) [6]. For low speed levels, f_r increases only slightly with speed, while at higher speed levels, f_r increases with almost the square of the speed [3]. At even higher speed levels a standing wave appears in the tire which greatly increases the energy loss and temperature rise in the tire, a condition that may eventually lead to tire failure [5], [3].

During estimations of vehicle performance or fuel economy, f_r is often assumed to be constant, with typical values around 0.011 to 0.015 for radial types representing passenger car tires on dry concrete or asphalt [5], [1] and [2].

2.7.3. Grading force

In case of a road grade (or inclination), the vehicle's dynamics will be affected by the component of the gravitational force F_g that is parallel with the road as

$$F_g = Mg \sin \alpha \quad (25)$$

where M (kg) is the vehicle mass, g (m/s^2) is the gravity constant, α (rad) is the road inclination angle.

$$\alpha = \arctan\left(\frac{\%grade}{100}\right) \quad (26)$$

Road slope is often expressed in terms of % grade, hence this terminology will be used throughout the thesis. Since the vehicle may be traveling uphill or downhill, this force may either be resisting or contributing to the net tractive force on the vehicle, i.e. it will either be positive or negative.

2.7.4. Wheel force

The tractive force, F_{wheel} that has to come to the wheels from the powertrain in order to sustain a certain speed level, road grade and acceleration can be found as in

$$F_{wheel}(t) = F_{acc}(t) + F_a(t) + F_r(t) + F_g(t) \quad (27)$$

Where F_{acc} (Nm) is the force required to accelerate the vehicle mass at a certain magnitude of acceleration ($F_{acc} = ma$).

A positive value of F_{wheel} then strives to accelerate the vehicle, while a negative value can represent either a regenerative braking force from an electric motor or friction braking.

The maximum tractive force on the driving wheels can be limited by either the powertrain's maximum force capability or the maximum adhesive capability between tire and ground that is possible to be applied on the wheel without loosing the grip to the road, i.e. starting to spin or slide [2]. The later is limited by the current normal force on the driving wheels, F_N and the coefficient of friction between the tire and the road, μ [1] as

$$F_{wheel,max}(t) = \mu F_N \quad (28)$$

The normal load on the driving wheels or wheel pair is affected by the weight distribution in the car, hence it varies from car to car, and even from occasion to occasion for the same car since the loading may vary, and finally by the change in weight distribution during an acceleration or deceleration, [1,2].The friction coefficient depends nonlinearly on the longitudinal tire slip, which is caused by deformation of the tire during acceleration and decelerations [1]. The slip is defined as

$$slip = \left(1 - \frac{v_{car}}{\omega r}\right) 100\% \quad (29)$$

and it leads to a non unity relation between the car speed, v_{car} (m/s) and the product of wheel speed ω (rad/s) and wheel radius r (m), which would otherwise be valid.

Starting from zero slip and friction, the friction coefficient increases with increasing slip, up to slip values of about 15 to 20% where the coefficient peaks at values around 0.8 to 1, depending on type of tire and road condition, [1] and [7]. At even higher slip values, the friction coefficient decreases, but at a lower rate than before. Moreover, high slip values means that the wheels, hence also the electric machine will spin faster than calculated directly from the vehicle speed while ignoring the tire slip

2.7.5. Wheel power and energy

The instantaneous tractive power that has to come to the wheels, P_{wheel} from the powertrain in order to sustain a certain speed level, road grade and acceleration is determined by the tractive force and the vehicle speed as

$$P_{wheel}(t) = F_{wheel}(t)v_{car}(t) \quad (30)$$

The total consumed energy at the wheel can be found from the time integral of the power as

$$E_{wheel} = \int P_{wheel}(t) dt \quad (31)$$

2.8 Vehicle performance

Basic vehicle performance includes maximum cruising speed, gradeability, and acceleration. The maximum speed of a vehicle can be easily found by the intersection point of the tractive effort curve with the resistance curve (rolling resistance plus aerodynamic drag), in the tractive effort vs. vehicle speed diagram shown in Figures 19-21. It should be noted that such an intersection point does not exist in some designs, which usually use a larger traction motor or a large gear ratio. In this case, the maximum vehicle speed is determined by the maximum speed of the traction motor as

$$V_{max} = \frac{\pi N_{m\ max} r_d}{i_0 30 i_{g\ min}} \quad (32)$$

where $N_{m\ max}$ is the allowed maximum rpm of the traction motor and $i_{g\ min}$ is the minimum gear ratio of the transmission (highest gear).

Gradeability is determined by the net tractive effort of the vehicle, $F_{t\ net}$, as shown in Figures 20-22. At mid- and high speeds, the gradeability is smaller than the gradeability at low speeds. The maximum grade that the vehicle can overcome at the given speed can be calculated by

$$i = \frac{F_{wheel} - (Fr + Fa + Fg)}{Mg} \quad (33)$$

Acceleration performance of a vehicle is evaluated by the time used to accelerate the vehicle from a low-speed V_1 (usually zero) to a higher speed (100 km/h for passenger cars). For passenger cars, acceleration performance is more important than maximum cruising speed and gradeability, since it is the acceleration requirement, rather than the maximum cruising speed or the gradeability, that dictates the power rating of the motor drive.

Chapter 3: Electric Motor Design-optimization Overview

3.1. Overview

Since its invention in 1820, the design methodology of the electric machine has gone through diverse stages to develop a fitting way to search for ideal design parameters.

Until 1979, the design of electric machines was implemented by an old, traditional design method that was dominated by the rule of thumb and historical empirical curves. Recent developments in power electronics, the generation of new magnetic materials, electric machine applications and manufacturing processes have stimulated the need to find a more efficient design methodology to convey these improvements.

Therefore, in this chapter, a comprehensive literature survey is introduced to summarise the traditional design method and the latest progress in optimisation of electric machines design.

3.2. Traditional method for electric machine design

The procedure of the traditional design method was governed by semi empirical sizing equations, a general, heuristic guideline and rule of thumb that predominantly reflect designer experiences.

The procedure is also based on a limited number of material curves that are not intended to be strictly accurate or reliable for every situation. After determining the machine electric and magnetic loading, the procedure is followed by iterative processes to tune some parameters, as shown in Figure 23 [5].

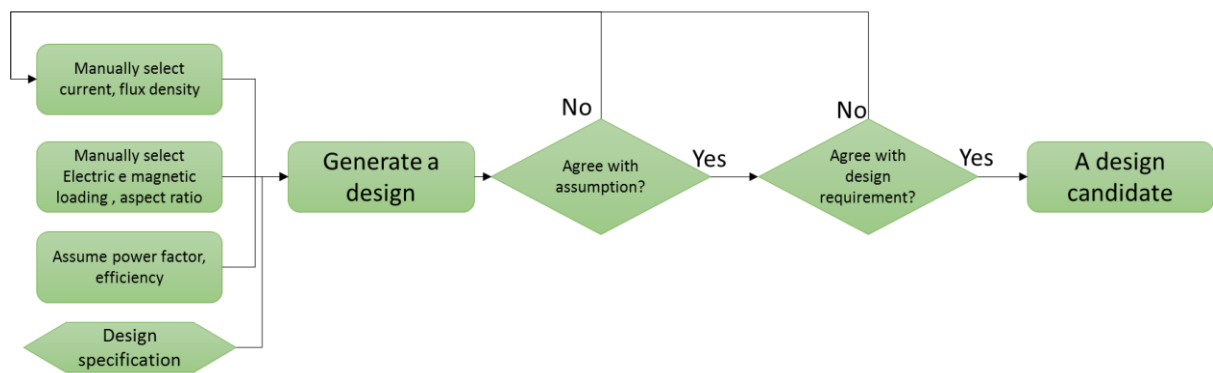


Figure 24 Illustration of the iterative design process in the traditional machine design

To achieve the required design outputs, the designer begins by selecting appropriate values for the main design dimensions as shown in the sizing equation (2.1) [6]

$$S = 11Kw \times \bar{B} \times ac \times D^2 L \times n \quad (34)$$

Where, S is the electric motor rating power (W), \bar{B} is the specific magnetic loading in Tesla (T), ac is the specific electrical loading in A/m , D is the stator inner diameter (m), L is the machine active length (m), Kw is the fundamental winding factor and n is the rated speed in revolution per second (rps).

According to the available cooling strategy, the designer estimates the values for the magnetic and electric loading. The selection of magnetic loading B depends on the saturation point and core loss of the available limitation materials, while the value of electric loading ac depends on the current density δ and type of winding insulation materials. Both B and ac values are selected from guidebooks based on common collected data and designers' experiences.

Upon selection of specific magnetic and electrical loading, the designer estimates the ratio between the stator inner diameter D and the machine active length L from the sizing equation (34). At this stage, the designer again needs to use an empirical curve and another sizing equation to approximate an appropriate number of pole-pairs p for the machine to calculate the machine aspect ratio λ , as shown in the Equation (35) .

$$\lambda = \frac{L}{\pi \frac{D}{p}} \quad (35)$$

However, the selection of aspect ratio λ based on Equation (35) cannot be useful in some applications where small machine outer diameter and high-power density are concerned. Furthermore, the determination of aspect ratio λ is not only limited by the parameters used in Equation (35), it is extended to include different machine variables, such as material utilisation, required performance, machine manufacturing feasibility, and cooling possibility.

After selecting the values for B , ac , p and λ and in order to determine the machine size, the designer needs to estimate another important factor, which is current density (J). In its simple form, current density is the amperes in conductor divided by the area of the conductor $J = I/A_{wire}$.

A higher value of current density increases copper losses and subsequently temperature rise. According to [10], the excessive current density in an electric machine is a common cause of electric machine failure. At rated current and high frequency, when the wire diameter is too small, the eddy current in the wire forces much of the current to flow near the outside of the conductor directly under the insulation. This can cause localised heating in the insulation, which may cause the insulation material to bubble-up and deteriorate the insulation system.

Furthermore, the limitation of current density between 5-7 A/mm² is valid only for air-cooling systems and does not reflect modern improvements where the current densities can increase sometimes up to 10 A/mm² for air cooling systems and up to 28A/mm² for liquid and gas cooling systems [9].

As mentioned before this process represent the old procedure, strongly related to the experience of the designer.

In the next chapter will be analysed the optimization procedure applied to the electric motor design that will become the core of this project.

3.3. Optimization of Electric Motor Design

The sophisticated nature of the electric machine makes the optimal design a difficult and challenging task. Electric machine design is concerned with paying particular consideration to machine weight, cost, volume and efficiency. The optimization problem of an electric machine involves continuous and discrete variables from different domains of physics that make the objective functions nonlinear and having no analytical expression [11].

Within the past decade, various optimization algorithms have been investigated for the design of electric machines. The main goal of these investigations was to find an ideal optimization method that could search for an optimum solution to all optimization problems. However, according to the “No Free Lunch Theorem”, if an algorithm performs well on a certain class of problems, then it necessarily pays for that with a degraded performance on the set of all remaining problems [12]. Therefore, there is no ideal algorithm that works perfectly for all optimization problems; instead, the proper optimization is the one that can efficiently survey all search space and find the optimal solution with a lower number of iterations. Thus, one of the main boundaries to utilizing design optimization is the difficulty in selecting the suitable optimization method for a given problem.

Generally, an optimization search procedure can be stated as finding the combination of independent variable parameters that maximize or minimize a given single or multi objective function, possibly subject to some constraints within the limited bounds for parameter [13].

Mathematically, the definition of the optimization procedure can be stated as followed[14,15]:

- Starting from the initial design parameter vector

$$\overline{X_0} = [x_{01}, x_{02}, \dots, \dots, \dots, x_{0D}], \overline{X_0} \in R^D \quad (36)$$

- Find the final design parameter vector

$$\overline{X_m} = [x_{m1}, x_{m2}, \dots, \dots, \dots, x_{mD}], \overline{X_m} \in R^D \quad (37)$$

- This satisfies the objective function set

$$f(\overline{X_m}) = [f_1(\overline{X_m}), f_2(\overline{X_m}), \dots, \dots, \dots, f_k(\overline{X_m})] \quad (38)$$

- And which subject to the design constraints

$$g_i(\overline{X_m}) \leq 0 \text{ For } i = 1, 2, \dots, \dots, n \quad (39)$$

- Where the boundaries of the design parameters are defined as

$$x_j^{(L)} \leq x_j \leq x_j^{(u)} \quad j = 1, 2, \dots, \dots, D \quad (40)$$

Based on these search criteria, several computational optimization techniques have been utilized and improved to solve engineering problems. Swarm Intelligence (SI) procedures that are based on population were the dominant means to search for an optimal solution to the design of electric machines.

3.3.1 Genetic Algorithm

In this research has been used the Genetic algorithms, GA developed by Holland [14] are adaptive algorithms based on the mechanism of natural selection and genetics for finding the global optimum solution for an optimisation problem [15]. Hence, when applied to optimisation problems, the GA has the advantage of performing a global search only. However, GAs have been widely used for solving complex electromagnetic problems and optimising final design behaviour of electric machines. The simple genetic algorithm is characterised by binary representation of individual solutions, crossover and mutation operators, and proportional selection rule. The standard procedure search of the genetic algorithm is outlined in Figure 25.

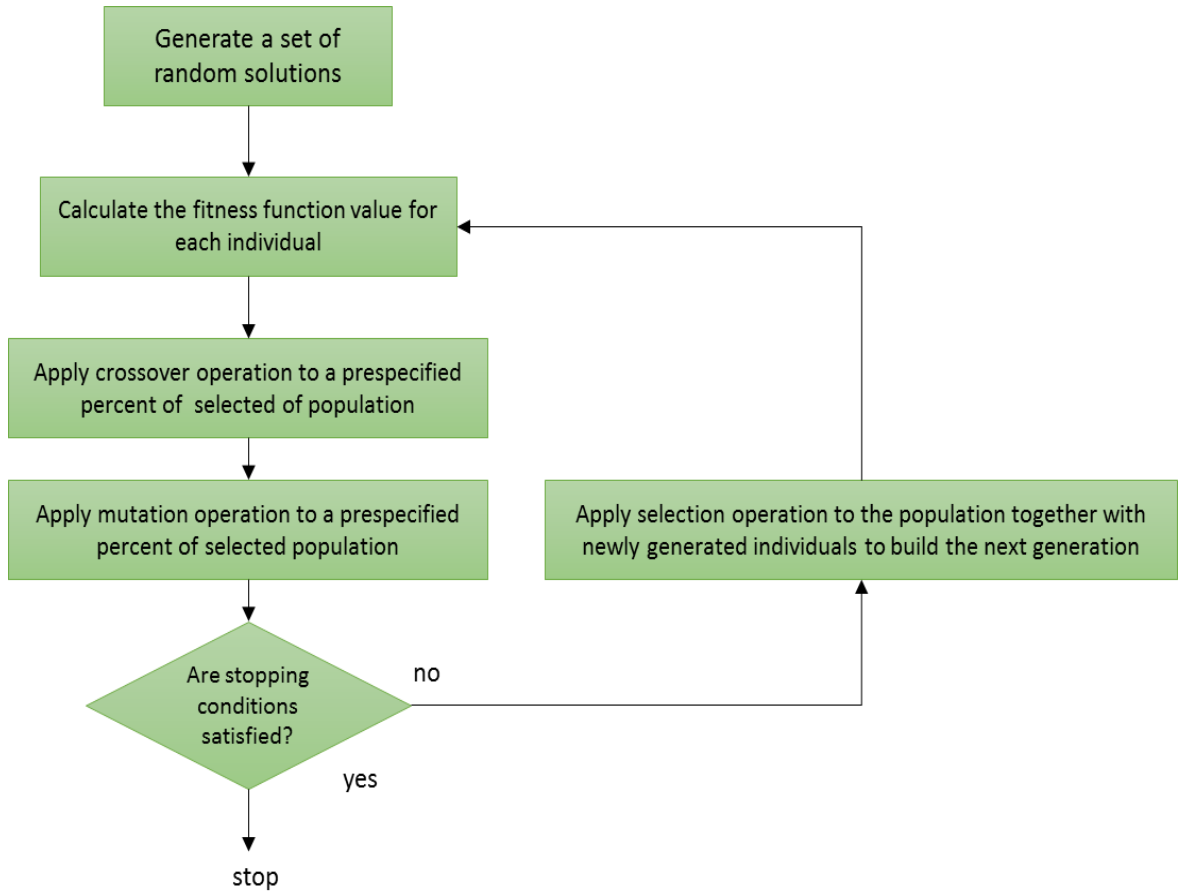


Figure 25 Standard search procedure of genetic algorithm

GA is a stochastic algorithm where population solution members are randomly initialised. The population members are encoded into binary representations called “strings” or “chromosomes”. The chromosomes are evaluated according to an objective function and a fitness score is assigned for each chromosome. At each cycle, the algorithm creates pairs of subset populations called “parents” and scales them into a raw fitness score; only the populations with higher/lower fitness values are chosen to pass to the next generation.

Chapter 4: Permanent magnet Synchronous Motor Design Optimization

In this chapter is explained the process that has been used to perform the optimization based on the three IPM configurations, and all the analysis done beyond that optimization.

Firstly, the base design used for the preliminary analysis and the training are introduced. Then, the design methodology used for the optimization of the three motors is explained. Finally, the sensitivity analysis done for each parameter involved in the optimization process is highlighted.

The sensitivity analyses are solved through Motor-CAD, whereas the optimization is performed through Motor-OPT(Optimization tool provided by MDL).

4.1. Definition of the base design

The brushless permanent magnet (BPM) machine of the 2012 Nissan LEAF is modelled in Motor-CAD; this design has been used as reference for the sensitivity analysis as well as for the optimization.

This motor will be called NISS1 during all the thesis.

The parameters that are highlighted in yellow have been considered fixed during the project.

The radial geometry of the stator has been set up as follows:

Stator Parameter	Value	Units
Slot Type	Parallel Tooth	-
Stator Ducts	None	-
Slot Number	48	-
Stator Lam Dia	198	mm
Stator Bore	132	mm
Tooth Width	4.15	mm
Slot Depth	21.1	mm
Slot Corner Radius	2	mm
Tooth Tip Depth	1.2	mm
Slot Opening	2.814	mm
Tooth Tip Angle	27	degrees
Sleeve Thickness	0	mm

Table 1 Stator parameters

The rotor magnet geometry has been set up as :

Rotor Parameter	Value	Units
Rotor Type	Interior V (web)	-
Pole Number	8	-
Notch Depth	-	-

Magnet Layers	2	-
L1 Magnet Thickness	3.862	mm
L1 Magnet Bar Width	13.9	mm
L1 Bridge Thickness	0.6	mm
L1 Web Thickness	21	mm
L1 Web Length	0	mm
L1 Pole V Angle	180	degrees
L1 Pole Arc	150	degrees
L2 Magnet Thickness	2.6	mm
L2 Magnet Bar Width	21.33	mm
L2 Bridge Thickness	7.65	mm
L2 Web Thickness	2.5	mm
L2 Web Length	0	mm
L2 Pole V Angle	124	degrees
L2 Pole Arc	159	degrees
Airgap	1	mm
Shaft Dia	44.45	mm

Table 2 Rotor Parameters

The axial dimensions of the motor have been set up as follows:

Axial Parameter	Value	Units
Motor Length	260	mm
Stator Lam Length	160	mm
Magnet Length	150	mm
Magnet Segments	18	
Rotor Lam Length	150	mm

Table 3 Axial Parameters

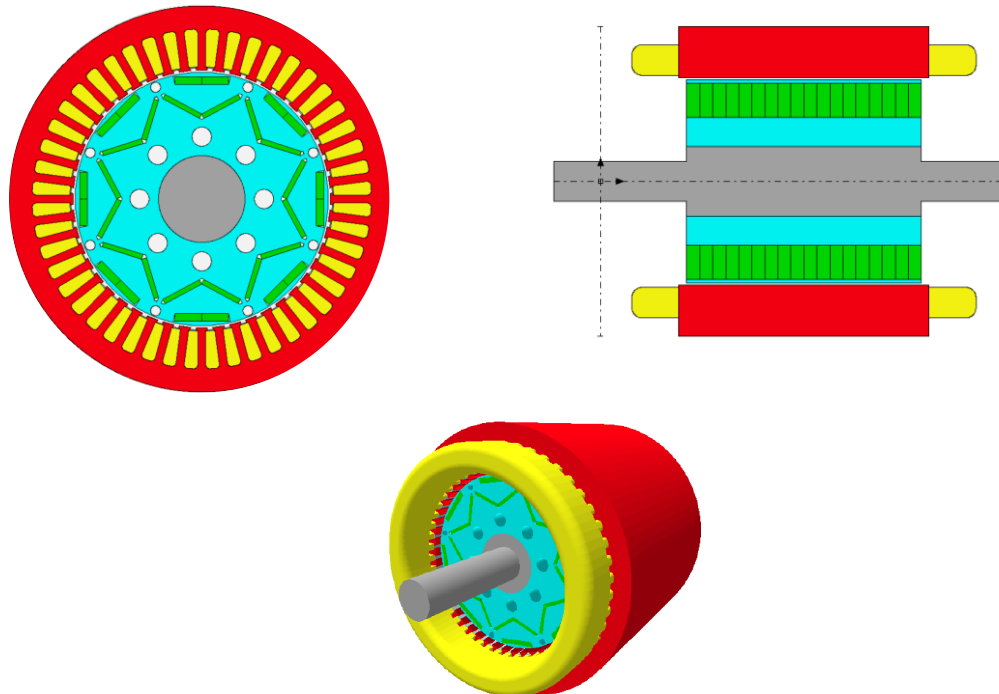


Figure 26 Motor Cad representation of NISS1 motor active parts.

Now that the geometry is defined, the conductors and the insulation inside the stator slots are considered. The electromagnetic winding definition starts with the configuration of the coils, their connection and the type of winding used in the design.

Parameter	Value
Winding Type	Distributed
Path Type	Central
Winding Layers	Single Layer
Phases	3
Turns	6
Throw	5
Parallel Paths	2

Table 4 Winding configuration

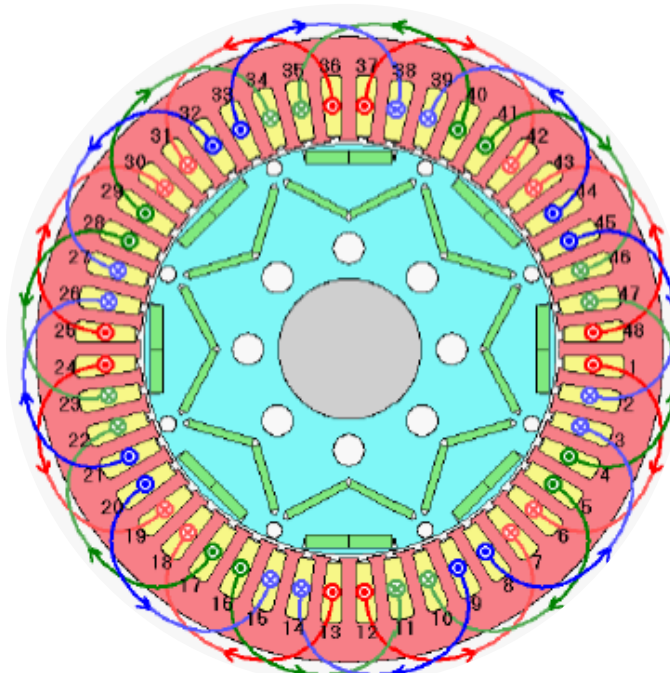


Figure 27 Winding configuration

Then the conductors have been characterized. Note that we have an overlapping winding since this design uses a distributed winding pattern.

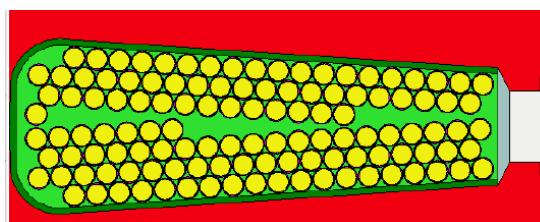


Figure 28 Wire configuration

Parameter	Value	Units
Winding Type	Overlapping	
Winding Definition	Wire Size	
Wedge Model	Wedge	
Wire Type	Metric Table	
Wire Gauge	[0.885mm, 0.800mm]	
Liner Thickness	0.25	mm
Copper Depth	100	%
Conductor Separation	0.02	mm
Number Strands in Hand	20	

Table 5 Wire configuration

The selection of materials plays a vital role in meeting the design specifications, which determine the performance, dimensions, weight, cost, and lifetime of the machines. In a typical IPM machine, both the rotor and stator cores are formed out of laminated silicon steel to effectively reduce the eddy currents and, hence, the iron losses. The properties of the silicon steel determine its mechanical strength, permeability, magnetic saturation, loss density, and thermal expansion.

In traction applications, non-oriented silicon steel is widely utilized as the core material due to its low cost, high yield and tensile strength, high saturation flux density, and low core loss. It is also possible to manufacture very thin laminations using non-oriented steel. In this research, M250 electrical silicon steel is selected as the core material for all three rotor topologies and stators.

Permanent magnets provide the magnetic torque component of the IPM machine. They contribute to higher torque density when compared to the other types of electric machines such as induction and conventional switched reluctance machines (SRMs). Magnets with higher remanence provide more torque while magnets with higher coercivity (absolute) value are less prone to demagnetization. In this design, Neodymium Iron Boron (NdFeB) based permanent magnets are selected because of their high remanence and relatively larger coercive force to achieve the best performance. Fig22 illustrates typical magnetic characteristics of a high-energy-density NdFeB permanent magnet.

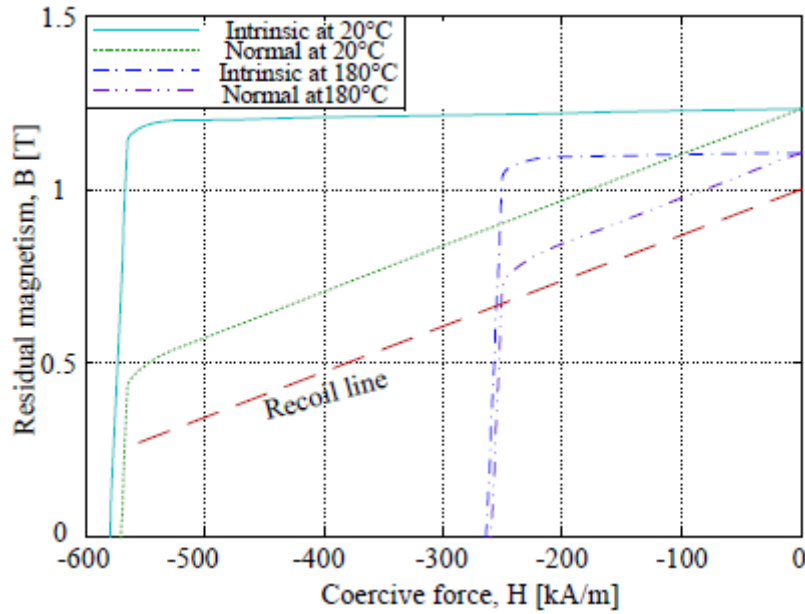


Figure 29 Magnetic characteristics of (N35) NdFeB grade

4.2. Design methodology

The way permanent magnets are embedded into the rotor laminations varies among different manufacturers, which considerably influences the machine performance. As described before, this thesis focuses on the design and comparison of the three IPM rotor topologies: the single V-shape, Flat-shape and Delta-shape. These three machine topologies follow the same design parameters targets and are subject to the same constraints.

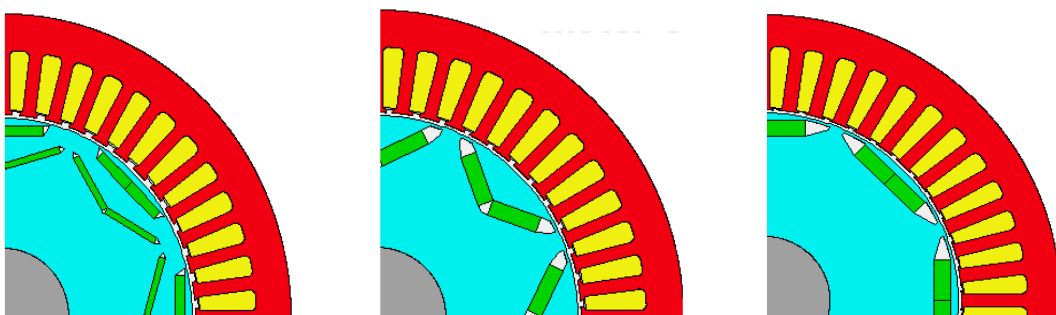


Figure 30 Cross section of "Delta shape"- "V shape"- "Flat shape"

The stator has three-phase distributed windings for 48 slots and 8 poles, which has been used in most of the commercial electrified vehicles. As described before, this project has been structured on the Nissan Leaf Electric motor specifications.

The process is based on the flowchart in figure 32:

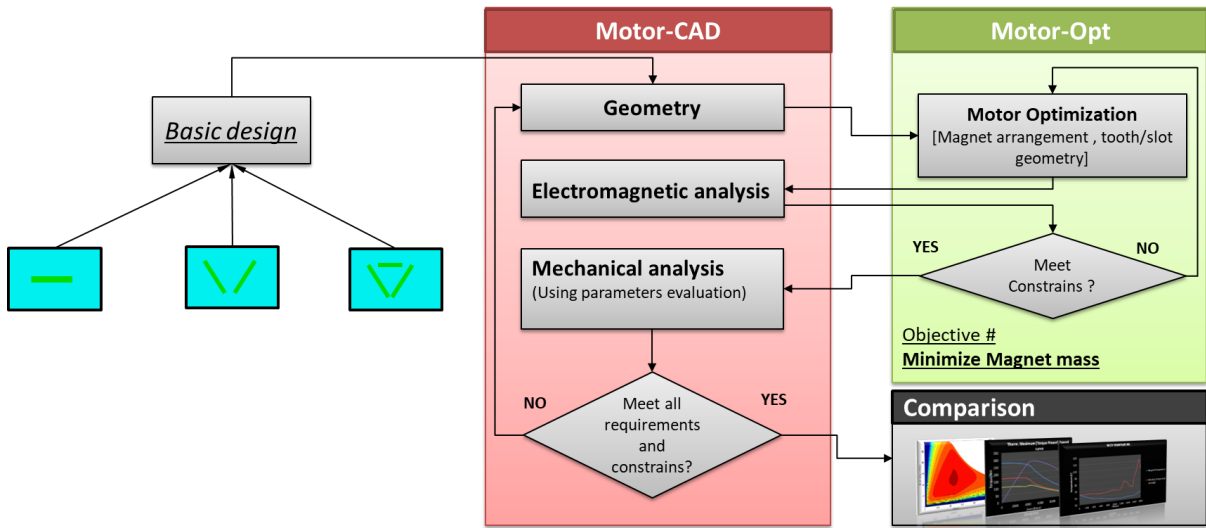


Figure 31 Design and optimization process

- 1) Basic design is generated based on the specifications described before. As already explained, three different arrangement are considered: FLAT-V-DELTA
- 2) Each design follows the same process, with different timing for the optimization, due to their intrinsic nature,
- 3) With Motor-OPT, the Parameters and the Constrains involved on the optimization have been selected,
- 4) The objective function is: Minimize magnet mass,
- 5) Each optimized design is analysed from mechanical and electromagnetic point of view after the optimization process,
- 6) Final comparison.

As said Motor-OPT is used to set up the optimization, during the process Motor-CAD performs a 2D FEA electromagnetic analysis for each design defined by Motor-OPT.

The qualitative aim of the optimization is to minimize the magnet mass at the base speeds. The aim is pursued by a single-objective optimization procedure.

The optimization is performed in the operating points corresponding to the values shown in table below.

Shaft speed [rpm]	DC bus [V]	Current Density [A/mm ²]
3800	375	17

Table 6 Operating point used during the optimization

Voltage values and current density are chosen according to the application. The design variables concern the stator and rotor core, the PM size and the stator slots. The rotor shape should be designed in order to have, in addition to the PM torque, a torque component due to the anisotropy of the rotor: an accurate design of the flux barriers can increase the difference between the reluctance of d-axis and q-axis, increasing the reluctance torque component and improving the motor performance when

it is driven at constant power over a wide speed range. The set of variables x used in the optimization procedure are listed in Tables below.

Rotor Parameter	Stator Parameter	Winding Parameter
R1- magnet thickness/Airgap	S1. Sloth depth /(Yoke th.+Slot depth)	W1.Phase in advance
R2. Magnet bar width/Mag. Thickness	S2. Slot opening /Slot width	-
R3. Bridge thickness	S3. Sloth width/slot pitch	-
R4. Pole V angle	-	-
R5. Web thickness	-	-
R6. Web length	-	-
R7. Pole arc	-	-

Table 7 Rotor/Stator/Winding Parameters involved in the optimization process

The design optimization needs to satisfy several constraints, as we said, in order to guarantee the reliability and feasibility of the final design. The considered constraints are listed in Table below.

Constraints	Value	Units
Minimum shaft torque	280	Nm
Minimum output power	130	kW
Maximum tooth flux density	1.9	T
Maximum yoke flux density	1.7	T
Maximum cost	500	-
Minimum efficiency	95	%
Maximum torque ripple	6	%

Table 8 Constraints involved in the optimization

The flux density value in the stator yoke is slightly higher than the typical values [9], but for the proposed applications it is reasonable thanks to the use of high permeability core material. The efficiency has been calculated as ratio between the output power and the output power plus the total losses.

Motor-Cad uses the magneto-static Finite Element analysis to evaluate the motor performance and the design requirements (at base speed), namely to compute the objective function value and constraints of the minimization problem which represents mathematically the optimal design problem. Motor-OPT defines the optimization procedure, it uses the information obtained by the FE program to iteratively update the set of motor parameters and try to identify an “optimal” motor by making a trade-off between the different parameters of the machine.

Before seeing the results of the optimization, it is interesting to review the study done as background of this optimization, each parameter involved has been treated separately with a “sensitivity analysis” in order to understand how it affects the performance of the motor.

4.3. Sensitivity analysis

Stator and Rotor parameters has been evaluated separately: NISS1 is the design used for this analysis, (One layer of magnet is considered)

This study has been performed through a tool of Motor-CAD called “sensitivity analysis”.

4.3.1. Rotor Parameters evaluation

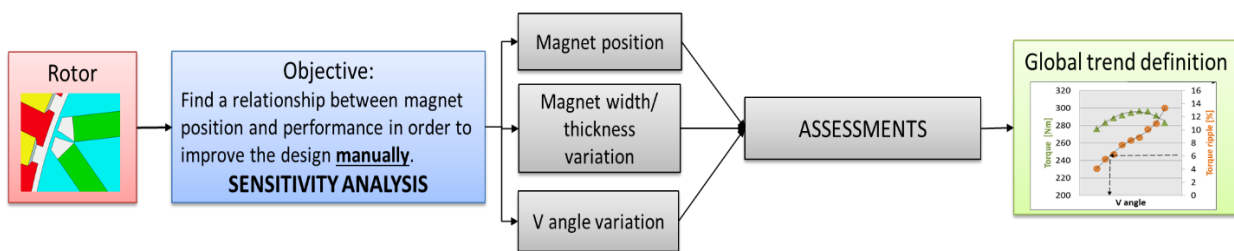


Figure 32 Rotor parameters evaluation

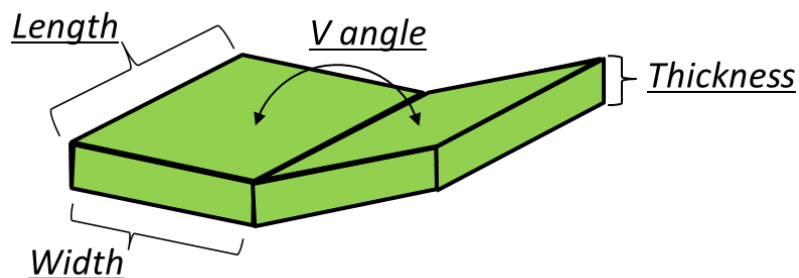


Figure 33 Rotor parameters

The operating point used for the analysis is characterized by the following value :

- Shaft speed [rpm]: 3800
- DC bus [V]: 375
- Peak current [A]: 480
- Phase advance angle [deg]: 40

a) Effect of magnet size on shaft torque

The first analysis is related on the magnet size. It is possible produce a magnet with the same mass but different aspect ratio ($Ar = \frac{width}{thickness}$), it has been evaluated the effect of different magnet mass with different aspect ratio on the shaft torque.

It has been used a V shape arrangement for the magnet in the rotor and all the other specifications follow the NISS1 design .

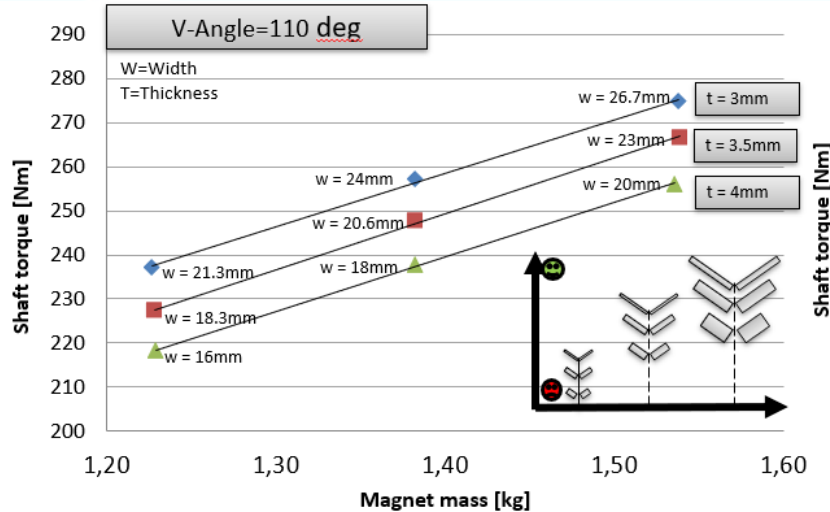


Figure 34 Effect of magnet size on shaft torque

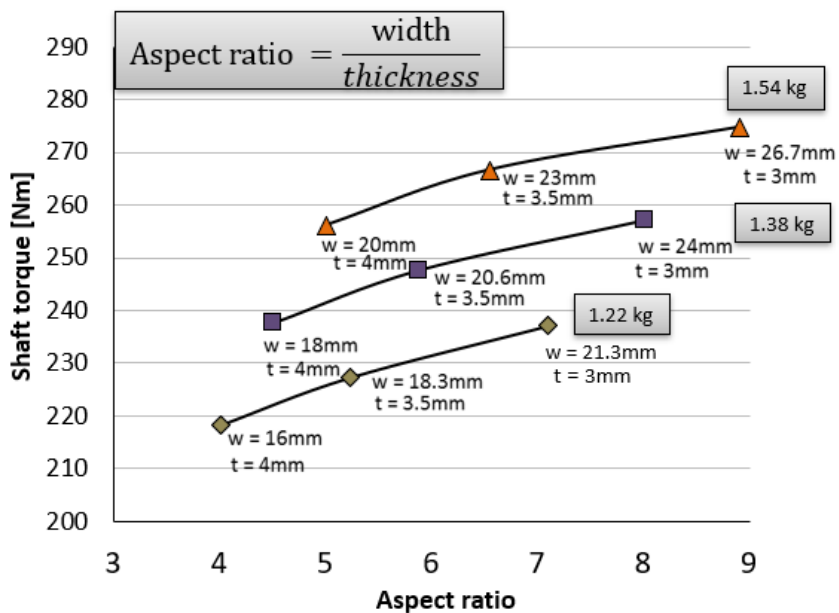


Figure 35 Effect of magnet size on shaft torque

- The thickness and width of the magnets affect the total magnet weight.
- The ratio between width and thickness [Ar] changes the flux distribution, maximum average torque and torque ripple.

Considering a fixed magnet mass, increase Ar means increase the average shaft torque

b) Effect of the magnet position on shaft torque and power

It has been used a V shape magnet configuration with the following characteristic :

- Magnet thickness= 4.1 mm
- Magnet width= 22 mm
- V-Angle= 110 deg

- Same operating point used before
- The rest of the motor follows the NISS1

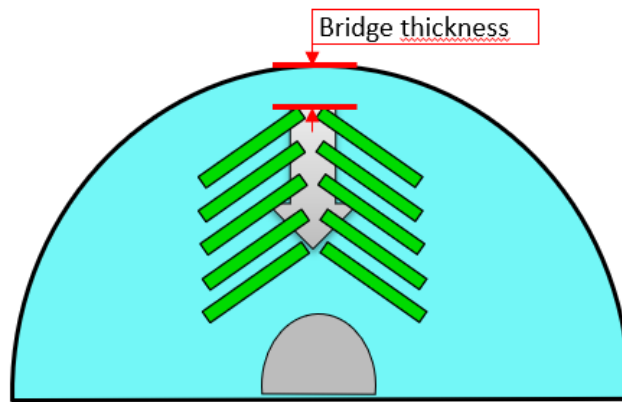


Figure 36 Magnet position

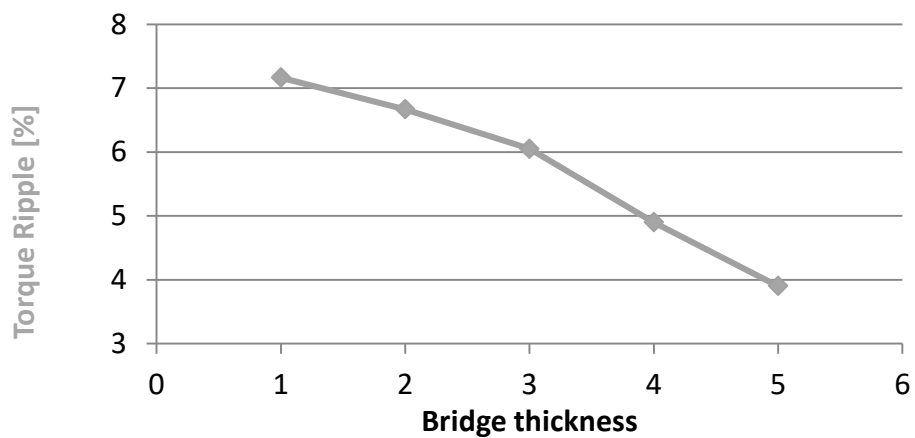


Figure 37 Effect of the magnet position on torque ripple

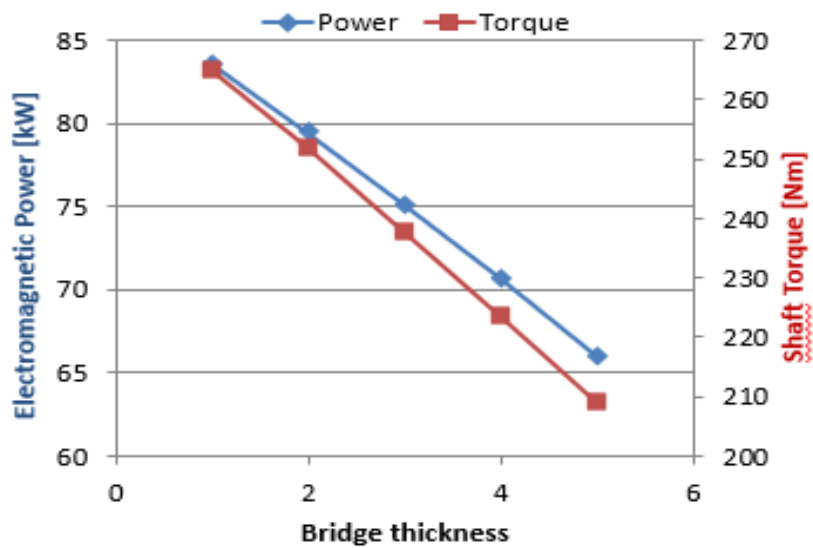


Figure 38 Effect of the magnet position on shaft torque and power

The Closer the magnets are to the outer rotor bore, the higher are the maximum average torque and torque ripple.

c) Effect of magnet V-angle on shaft torque and torque ripple

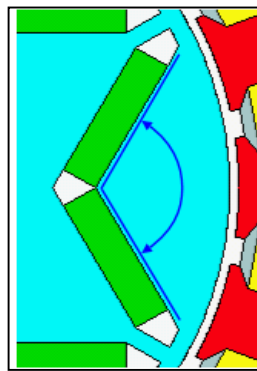


Figure 39 Magnet V-angle

It has been used a V shape magnet configuration with the following cartelistic :

- Magnet thickness= 4.1 mm
- Magnet width= 22 mm
- Same operating point used before
- The rest of the motor follow the NISS1

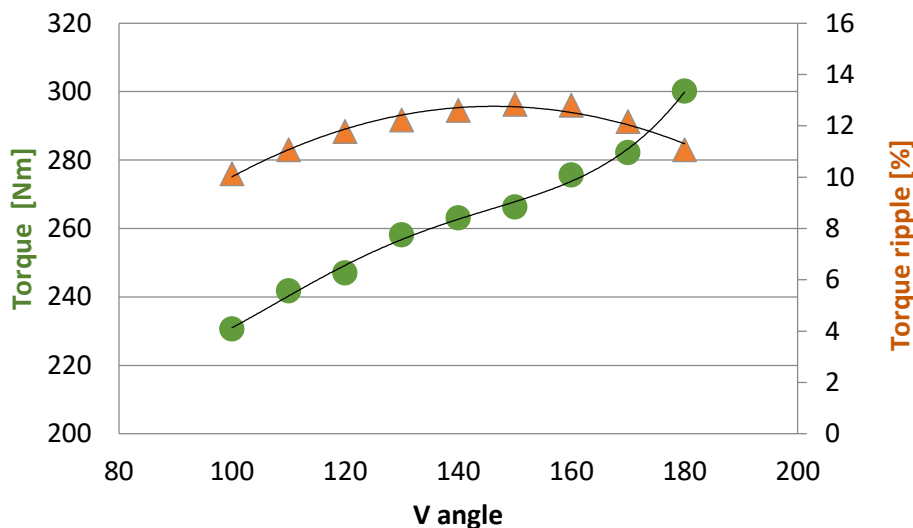


Figure 40 Effect of magnet V-angle on shaft torque and torque ripple

➤ The angle between two magnet changes the maximum average torque and the torque ripple.

The torque ripple increases with the V angle until 150°, after that value it decreases.

4.3.2. Stator parameters evaluation

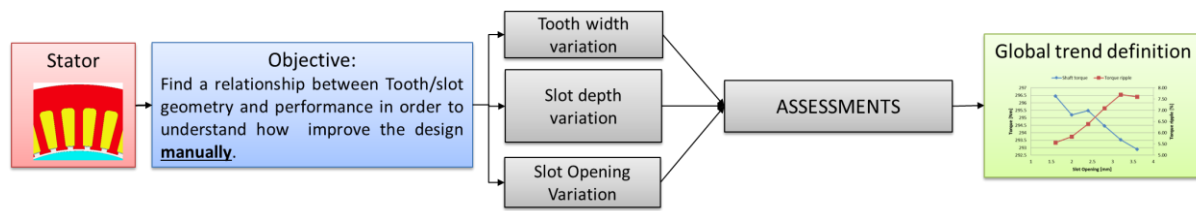


Figure 41 Stator parameters evaluation

It has been used the same operating point defined for the rotor parameters analysis.

The rotor configuration is the one used in the NISS1.

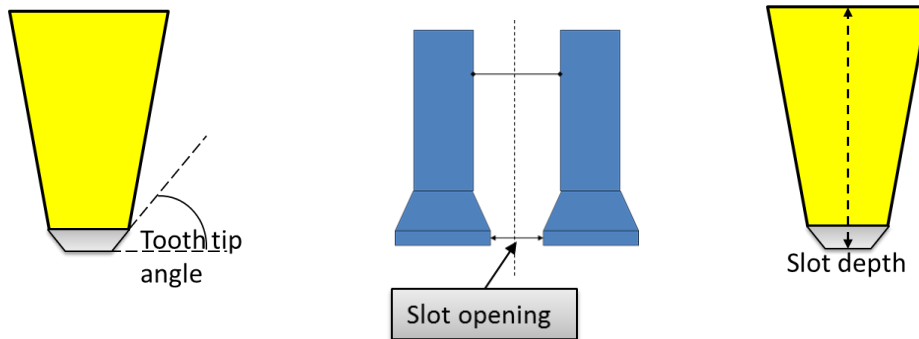


Figure 42 Stator parameters

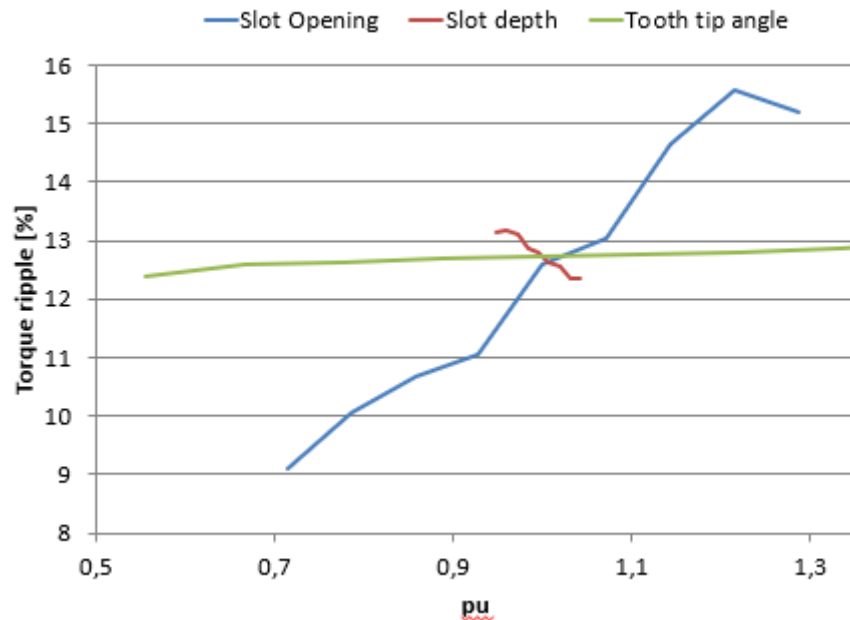


Figure 43 Effect of Slot Opening , Slot depth and Tooth tip angle on torque ripple

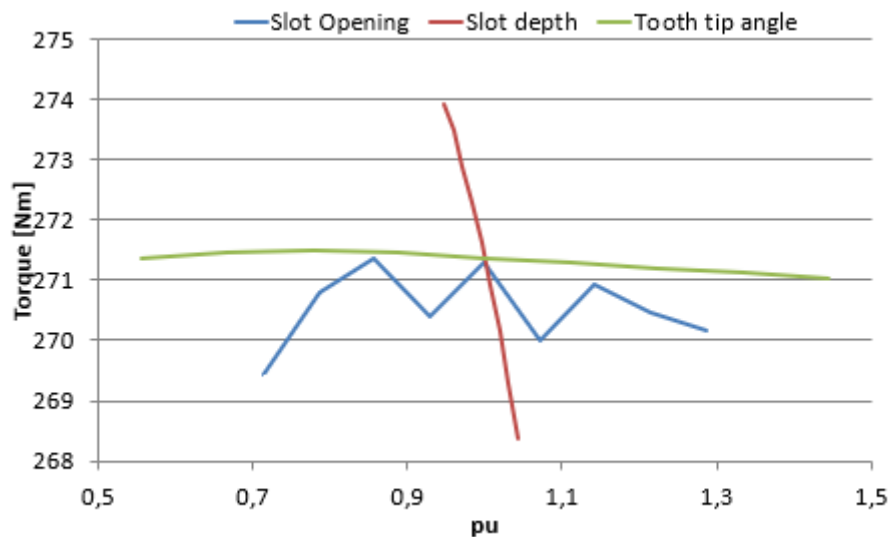


Figure 44 Effect of Slot Opening , Slot depth and Tooth tip angle on torque

- The torque is slightly affected by the Slot depth.
- The torque ripple is mainly affected by the slot opening.

Chapter 5: Optimization results

After the preliminary analysis, it has been performed the optimization for the 3 different magnet arrangement.

5.1. Flat-shape

The optimization of the Flat-shape design for a single operating point took 3 days of simulation.

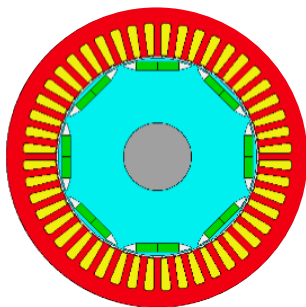


Figure 46 Flat-shape Base design

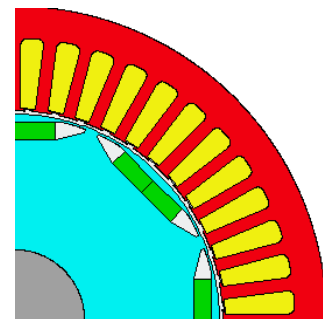


Figure 45 Flat-shape Optimized design

	Unit	Base Design	Optimized design
Magnet mass	kg	1.56	1.37
Electromagnetic Power	kW	131	148
Electromagnetic torque	Nm	320	331
Torque ripple	%	4.9	5.2
Phase in advance	deg	40	49

The magnet mass has been reduced by 13% respect to the Flat-shape base design, mainly due to the reduction of the magnet width. The optimized design present a reduction of the magnet width , the performance of the motor overcomes the requests.

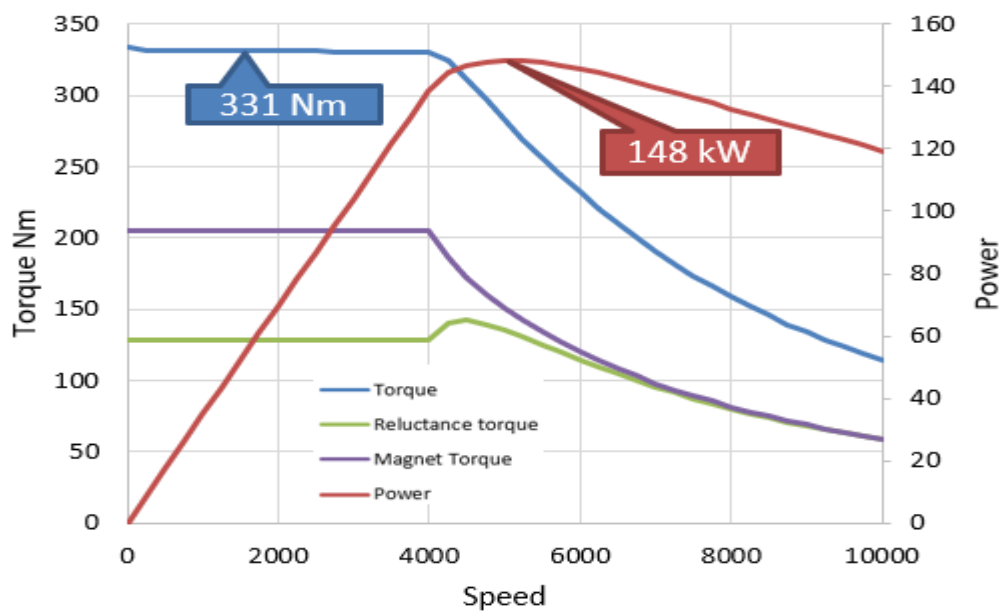


Figure 47 Maximum torque and power versus speed profiles of the optimized flat-shape design

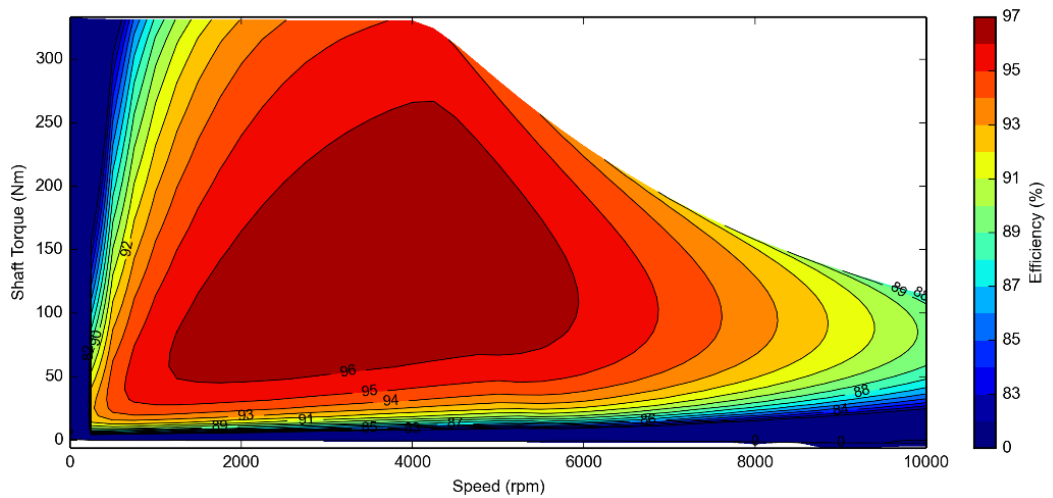


Figure 48 Flat-shape Efficiency

5.2. V-shape

The optimization of the V-shape design for a single operating point took 6 days of simulation.

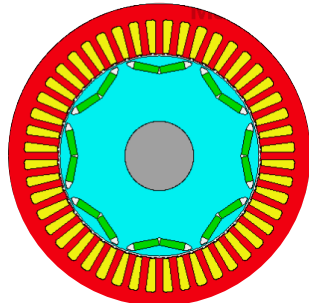


Figure 49 V-shape Base design

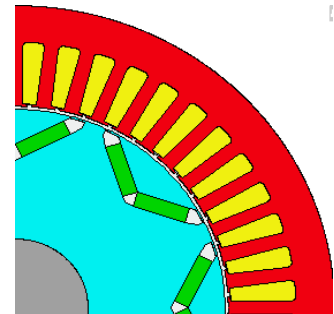


Figure 50 V-shape Optimized design

	Unit	Base Design	Optimized design
Magnet mass	kg	1.6	1.57
Electromagnetic Power	kW	131	133
Electromagnetic torque	Nm	320	331
Torque ripple	%	4.9	5.2
Phase in advance	deg	40	50.2

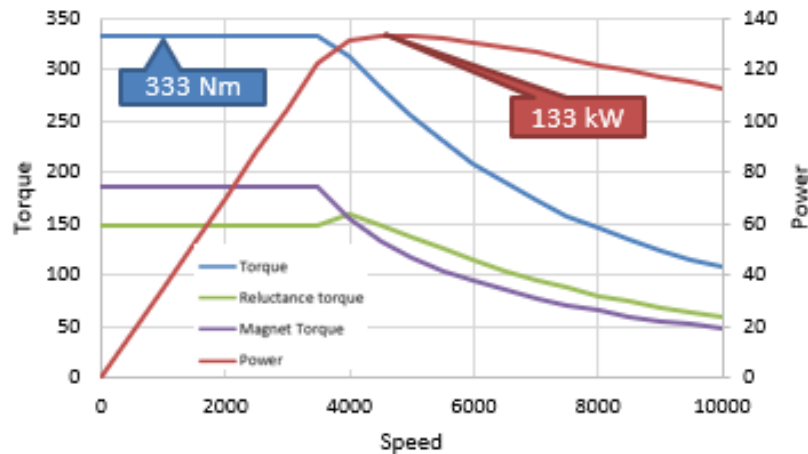


Figure 51 Maximum torque and power versus speed profiles of the optimized V-shape design

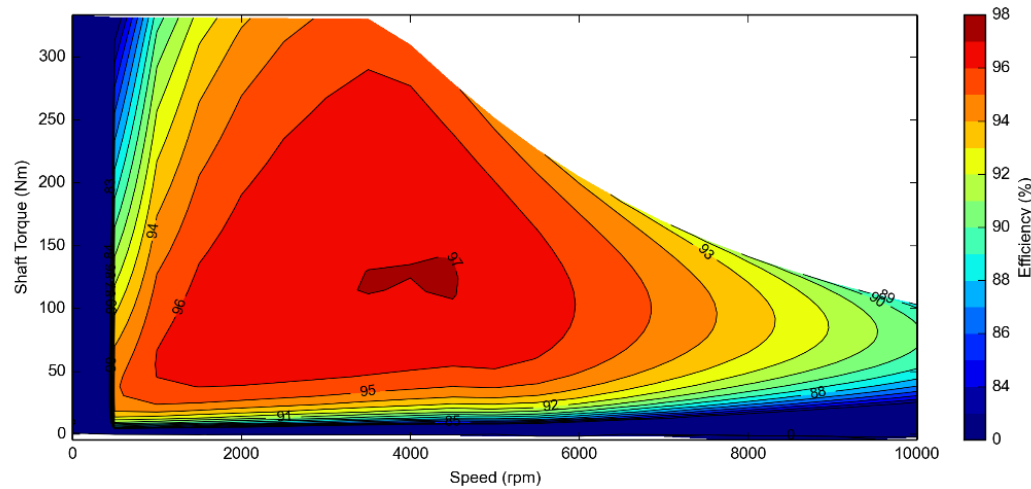


Figure 52 V-shape Efficiency

5.3. Delta-shape

The optimization of the Delta-shape design for a single operating point took 6 days of simulation.

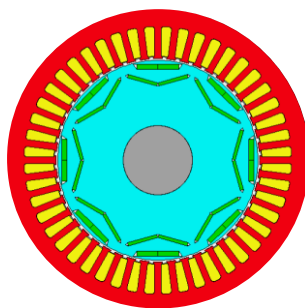


Figure 54 Delta-shape Base design

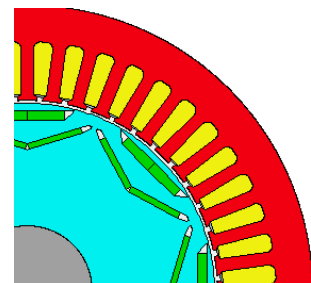


Figure 53 Delta-shape Optimized design

	Unit	Base Design	Optimized design
Magnet mass	kg	1.66	1.6
Electromagnetic Power	kW	130	131
Electromagnetic torque	Nm	325	350
Torque ripple	%	4.9	6
Phase in advance	deg	40	46.3

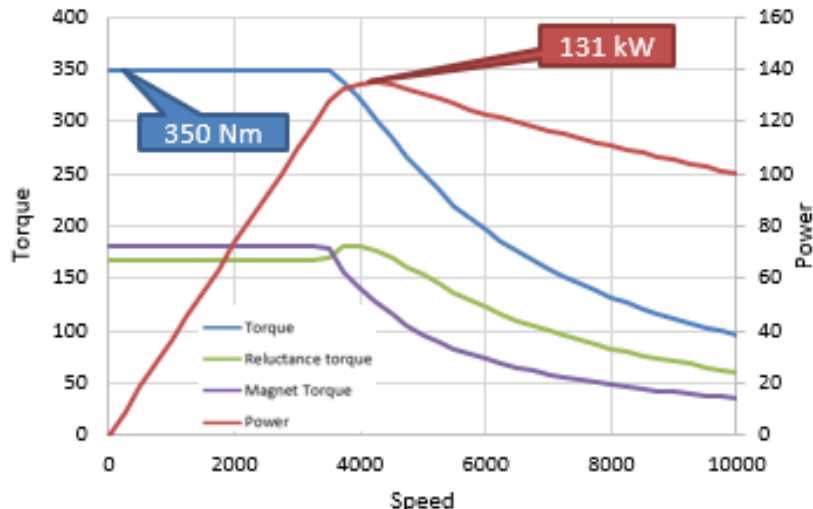


Figure 55 Maximum torque and power versus speed profiles of the optimized Delta-shape design

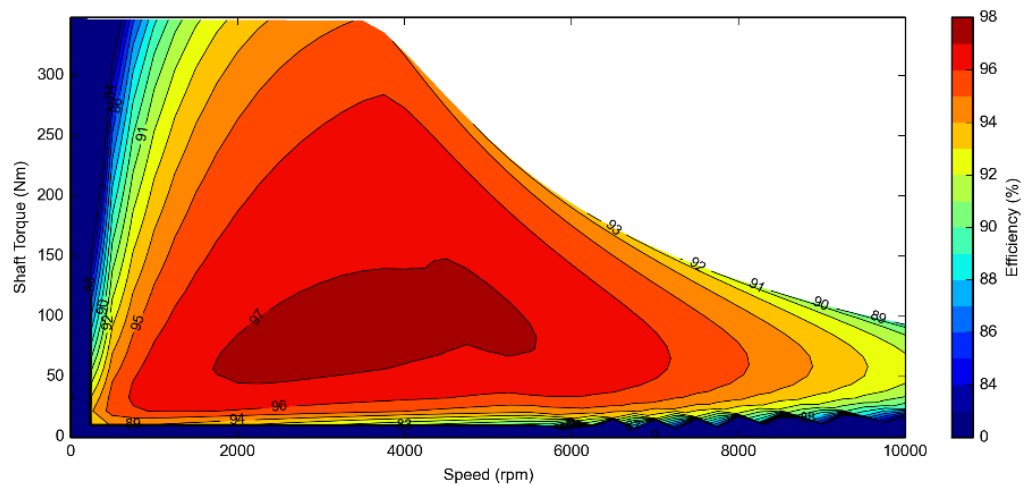


Figure 56 Delta-shape Efficiency

5.4. Comparison

Finally it is possible to compare the three different design analysed.

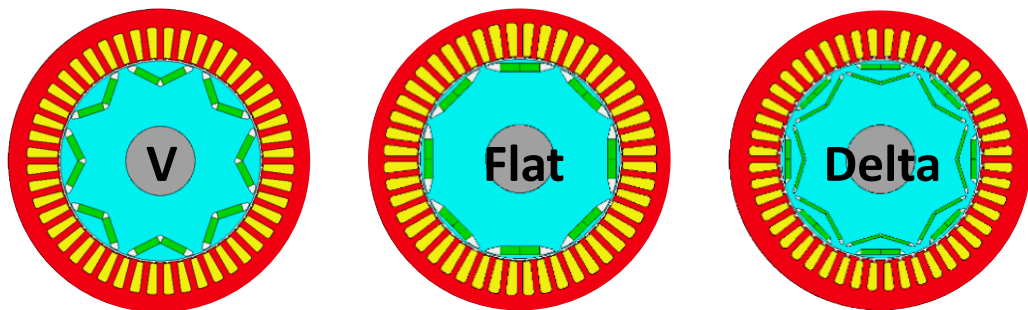


Figure 57 Optimum design

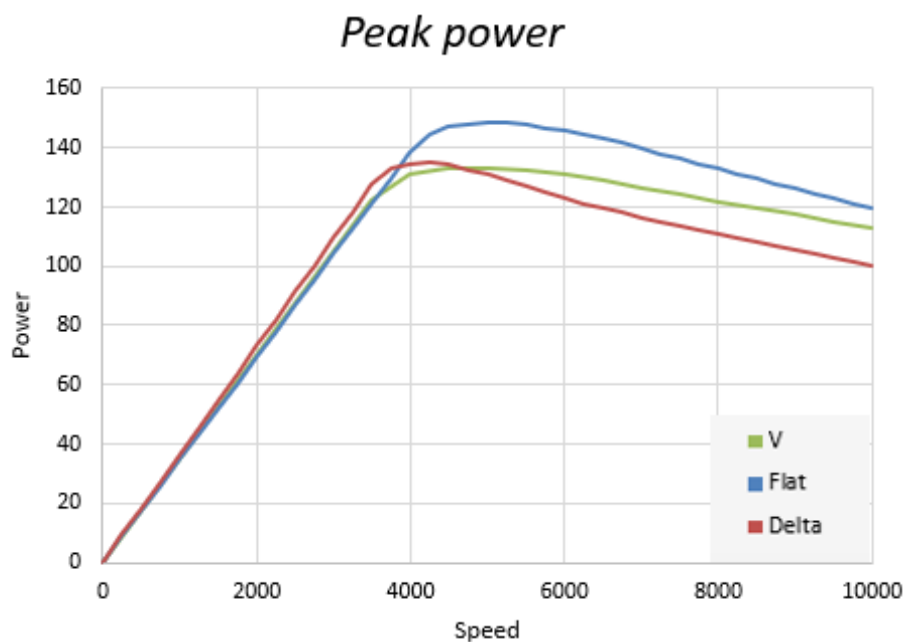


Figure 58 Maximum power versus speed profiles of the optimized design

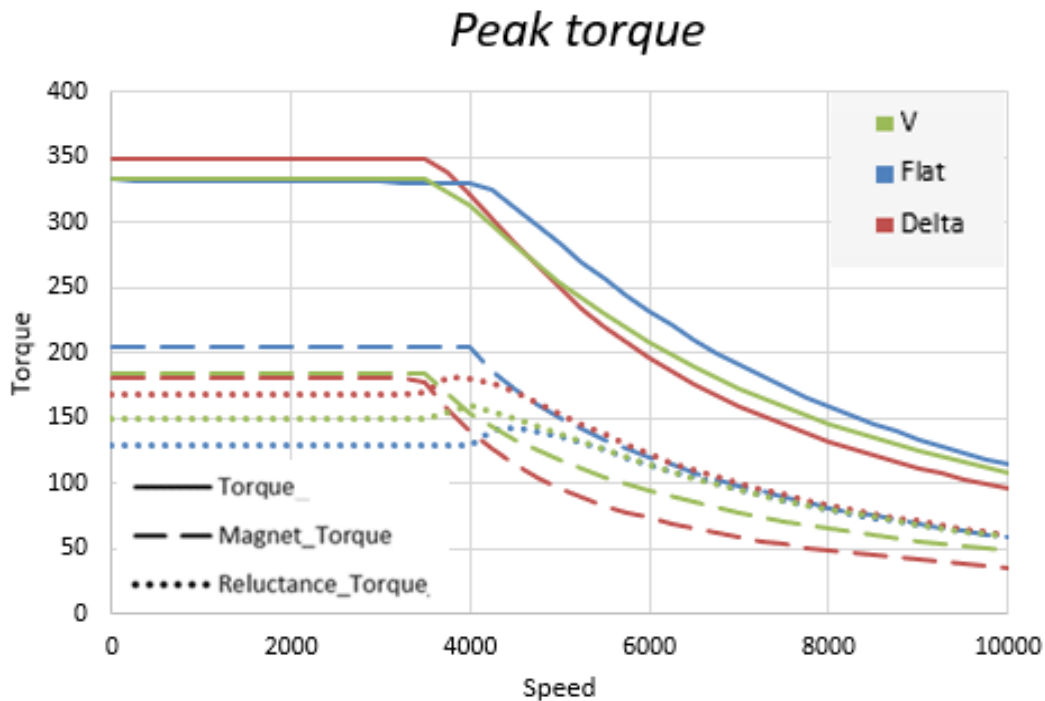


Figure 59 Maximum torque versus speed profiles of the optimized design

- Flat shape has the smallest amount of magnet.
- Flat presents the highest peak power.
- Delta has the highest torque and the highest **reluctance torque and the best efficiency map**.

The optimization involves a limited number of parameters (Motor-opt cannot include the geometry of the flux barrier ex.). Given the intrinsic geometry of the Flat-shape design (rectangular magnet), the optimization has been done by the software considering $\approx 80\%$ of its geometric parameters.

The Delta-shape design cannot be tuned as much as the Flat one, due to its more complex structure.

Even though the Delta-shape design presents some limitations, as mentioned above, it remains the shape with most potential for improvement.

Chapter 6: Vehicle analysis results- optimal gear ratio

Traction motors as we have seen should meet requirements such as high instantaneous power, high power density and high torque at low speed for starting and climbing. Apart from the traction motor, another important component related to power performance is the transmission or gearbox in the drive system of the vehicle.

Commonly, relative to the gear ratio selection, electric vehicles, utilize either single ratio transmissions or direct drive with no gear reduction in delivering the traction load to the road. Consequently, the gear ratio design needs to achieve a balance between the range, performance, and top speed. The appropriate gear sizing affects the overall efficiency by effecting motor efficiency.

In this chapter it has been analysed the vehicle in order to define the optimal gear ratio applicable.

Considering a fixed vehicle, the gear ratio will affect the size/cost of Electric Motor, Inverter and Transmission. The table below explain perfectly the concept.

Gear ratio (example)	Peak Torque of the motor	Peak Current of the motor (losses)	Size and weight of the motor	Cost
1	↑	↑	↑	↑
10	↓	↓	↓	↓

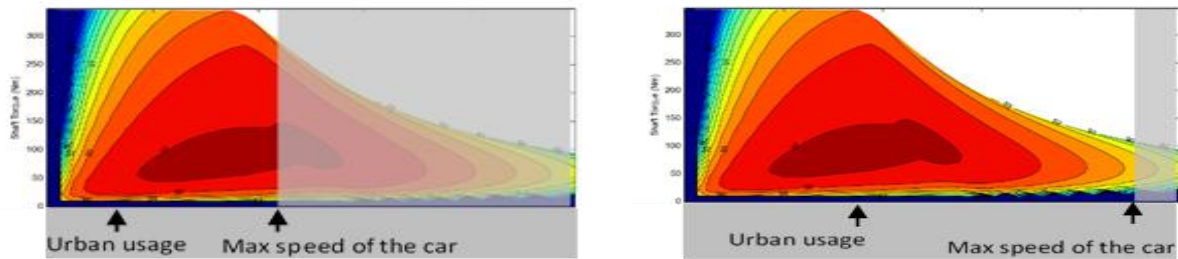
Table 9 Gear ratio example

A gear ratio equal to 1 means that there is a direct connection between wheels and the electric motor.

$$T_{wheels} = T_{electric\ motor} \quad (41)$$

If on the one hand we have saved the cost of the transmission , to the other we have significantly increase the size of the motor (more magnet) and the size of the inverter.

The cost of the transmission is certainly lower than the cost of the enlargement of the powertrain components. It is recommended use the maximum gear ratio allowed in order to minimize the size of the motor and then minimize the cost of it.



Another aspect that we have to consider is the usage of the electric vehicle. The vehicle that is considered in the project has a maximum speed of 150 kmph and the electric motor can achieve an maximum angular velocity of 10000 rpm. These two value will characterise the optimal gear ratio for this specific application. In term of usage, we would like to fix the maximum speed of the car in order to achieve the maximum efficiency of the motor during the urban usage. (see the figure below)

The gear ratio is defined by different vehicle performance:

- Gradeability
- Top vehicle speed
- 0-100 kmph

In this project , as said before the maximum rotational speed of the electric motor is fixed, 10000 rpm.

$$\text{Max speed of car} = 150 \text{ km/h} = 1326 \text{ rpm (@wheel)} \quad (42)$$

$$\frac{\text{Max speed of the motor}}{\text{Max speed of the car}} = \frac{10000}{1326} = 7.5 \text{ Max gear ratio allowed} \quad (43)$$

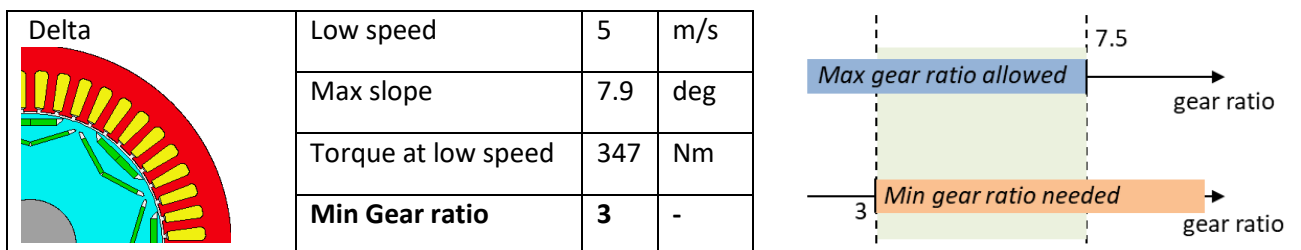
Since the maximum speed of the car and the maximum speed of the motor are the same for each permanent magnet electric motor the max gear ratio allowed is the same as well.

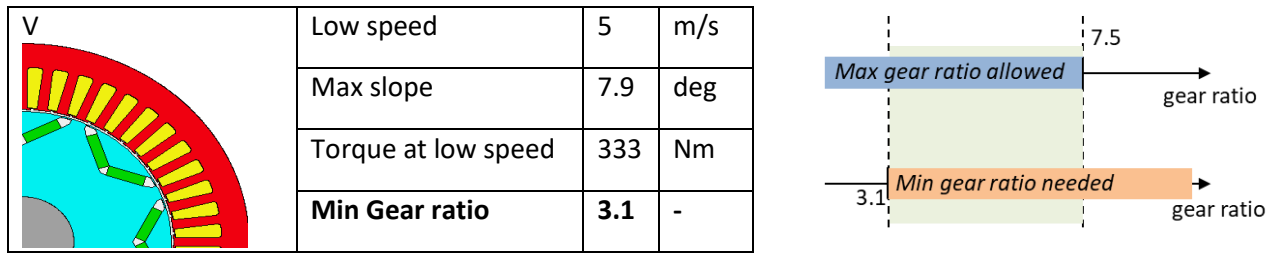
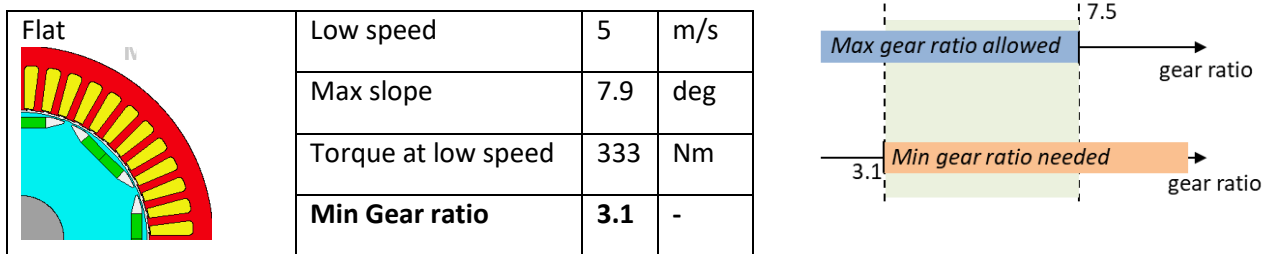
To the other hands, the Gradeability test will be affected from the maximum torque achieve from the motor.

$$\frac{i_g \eta_t T_p}{r_d} \geq M g f_r \cos \alpha + \frac{1}{2} \rho_a C_D A_f V^2 + M g \sin \alpha$$

Parameters	Explanation	Value	Units
η_t	Efficiency of the driveline	0.8	
T_p	Torque output from the electric motor	-	Nm
M	Total mass of the vehicle(curb weight + passengers)	1821	Kg
g	Acceleratio constant	9.8	m/s^2
f_r	Rolling resistance coefficient	0.017	
ρ	Density of air	1.225	Kg/m3
V	Vehicle speed	5	m/s
i_g	Gear ratio		
α	Slope	20	
C_d	Drag coefficient	0.28	m
A_f	Vehicle frontal area	2.29	m^2
n_{pmax}	Limitation in max rpm of the EM	10000	rpm

6.1. Gradeability test





The gear ratio will be the maximum allowed, then as explained will be the same for each motor.

6.2. Optimal Gear ratio

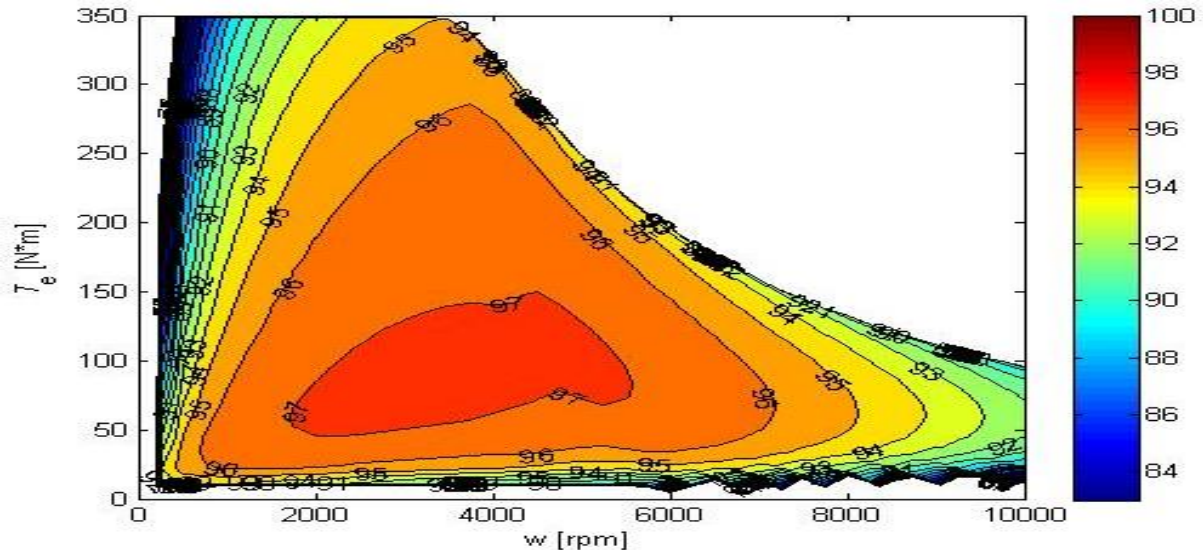


Figure 60 Delta-shape Efficiency

The EV considered in this thesis, as explained before is characterized by a single gear ratio, as the majority of the electrical vehicle in the market.

The gear ratio will affect the average efficiency of the electric motor during a certain drive cycle and the performance of the vehicle as well.

From the picture above is possible to see that an higher gear ratio ,considered an equal max speed of the vehicle , will fix the max speed of the EM to the right side of the graph and as consequence an smaller value will move the max speed of the EM to the left side.

Considering as example the Delta design, it has been defined 3 gear ratio value in order to compare in terms of speed ,acceleration and drive cycle performance the optimum value.

Gear ratio: 3, 5 ,7.5



Figure 61 Effect of the gear ratio on the speed of the car

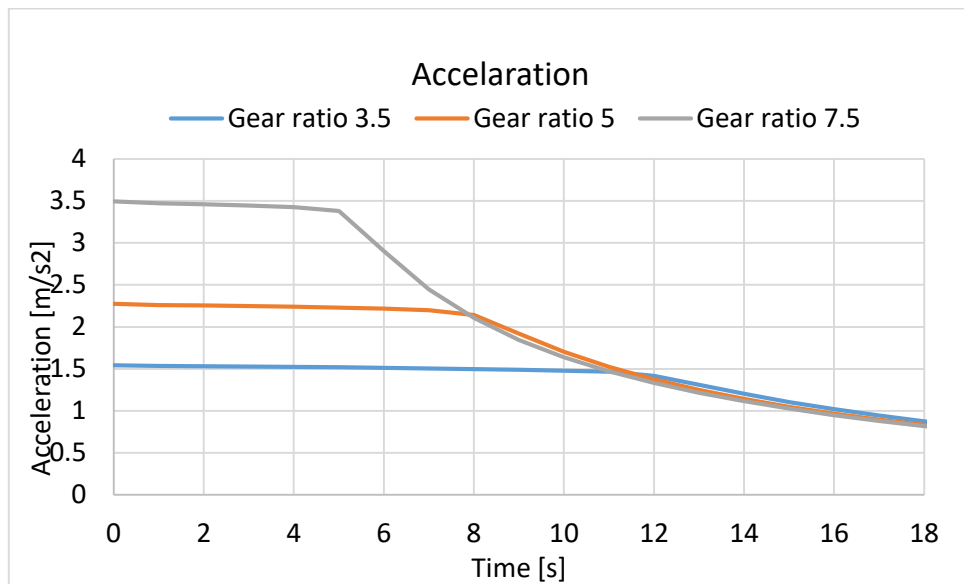


Figure 62 Effect of the gear ratio on the acceleration of the car

WLTP	Unit	Delta shape		
Gear ratio	-	3.5	5	7.5
Average Efficiency	%	91.4	90.1	86.9
Total loss (Electric Motor)	Wh	218	234	377

As Expected and higher Gear ratio allow to reach higher acceleration value. It has been also performed a comparison due to the drive cycle WLTP. This analysis is performed with the software used for the design of the EM , Motor-CAD.

As expected, from the efficiency point of view we reach a better value with the lowest gear ratio, but the optimal value need to take care also of the performance of the car and the potentiality of the EM.

Then the conclusion is that it has been chosen the highest value in order to provide the best performance of the vehicle, in line with the car sector expectation .

6.3. Results and Comparison

The purpose of this thesis is to show the evolution of the Electric motor used in EV in terms of magnet design. In order to provide a correct scenario, has been selected the optimul gear ratio for each EM with the characteristic magnet arrangement. In this chapter will be first described each result separately and finally there will be a comparison.

Magnet Shape	Gear ratio	0-100 kph	Average efficiency (WLTP)
Flat	7.5	8.5 sec	86.9%

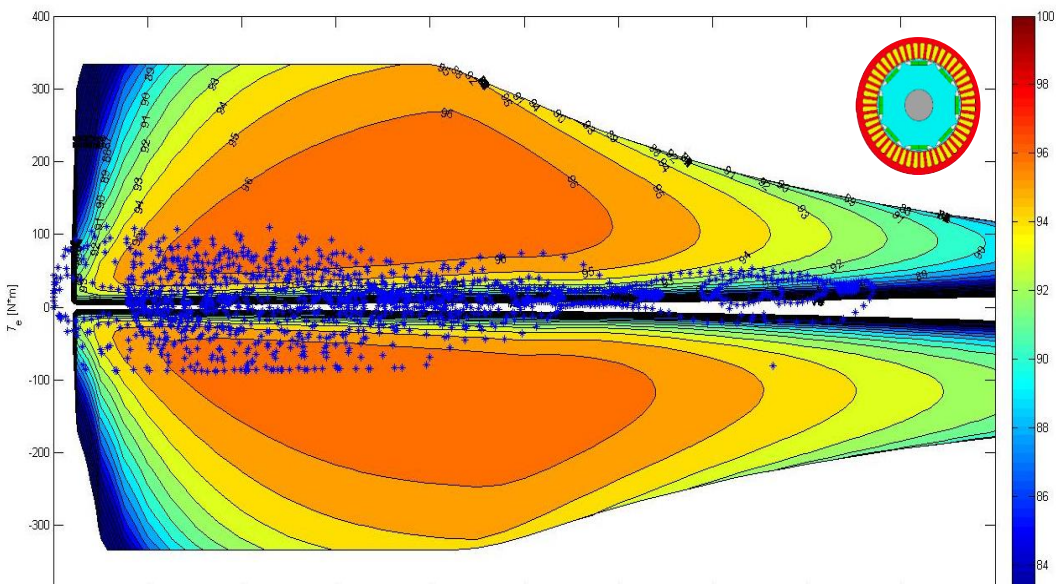
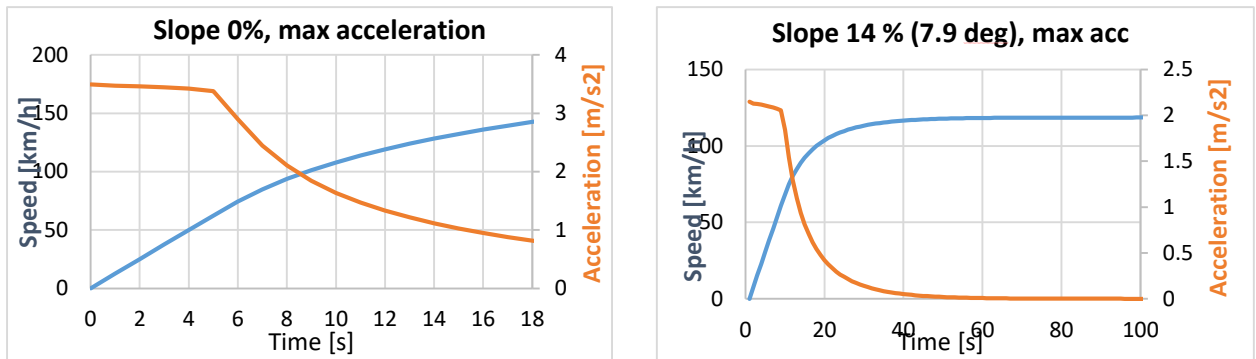


Figure 64 Flat-shape Efficiency



The graph above represents the efficiency map of the EM with the Flat magnet shape on which are printed the point of the drive cycle WLTP.

The performance of the m vehicle is described by the time that the vehicle require to go from 0 to 100 kmph, to the other hands the purely performance of the motor it has been described by the average efficiency of the EM during that drive cycle.

In addition it has been performed an acceleration test with no slope and with the max slope usually used by the car maker (7.9deg)

This analysis will be performed also for the other 2 magnet dosing.

Magnet Shape	Gear ratio	0-100 kph	Average efficiency (WLTP)
V	7.5	9.2 sec	87.56

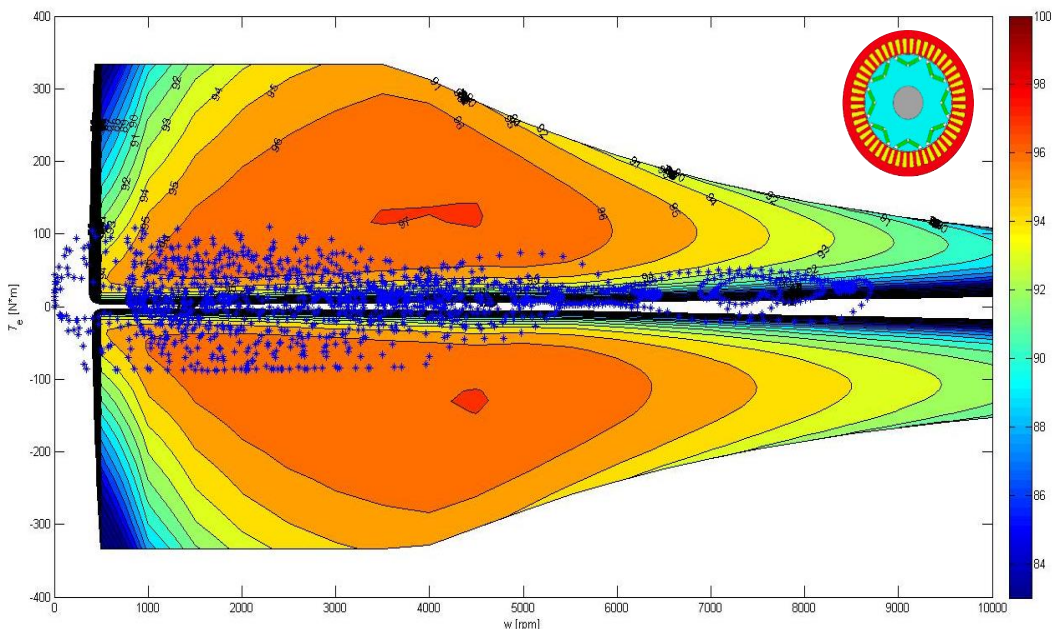
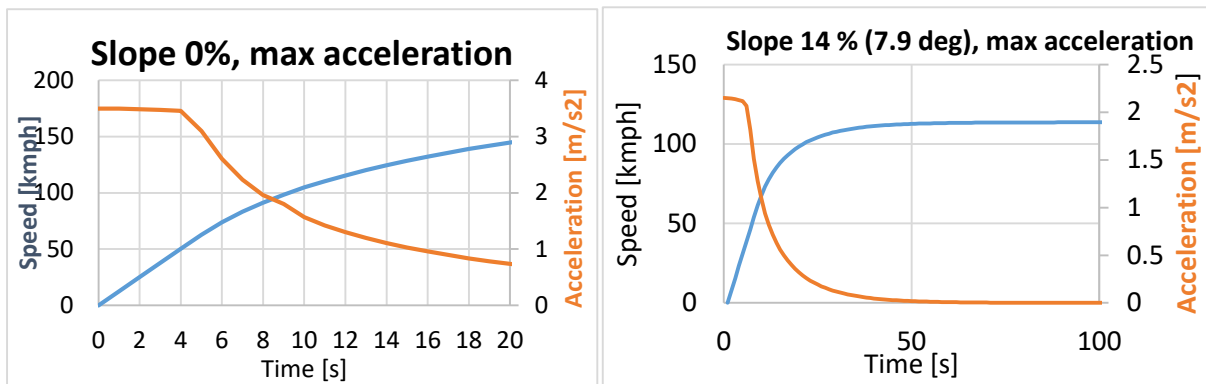


Figure 65 V-shape Efficiency



Magnet Shape	Gear ratio	0-100 kph	Average efficiency (WLTP)
Delta	7.5	9.1	91.8

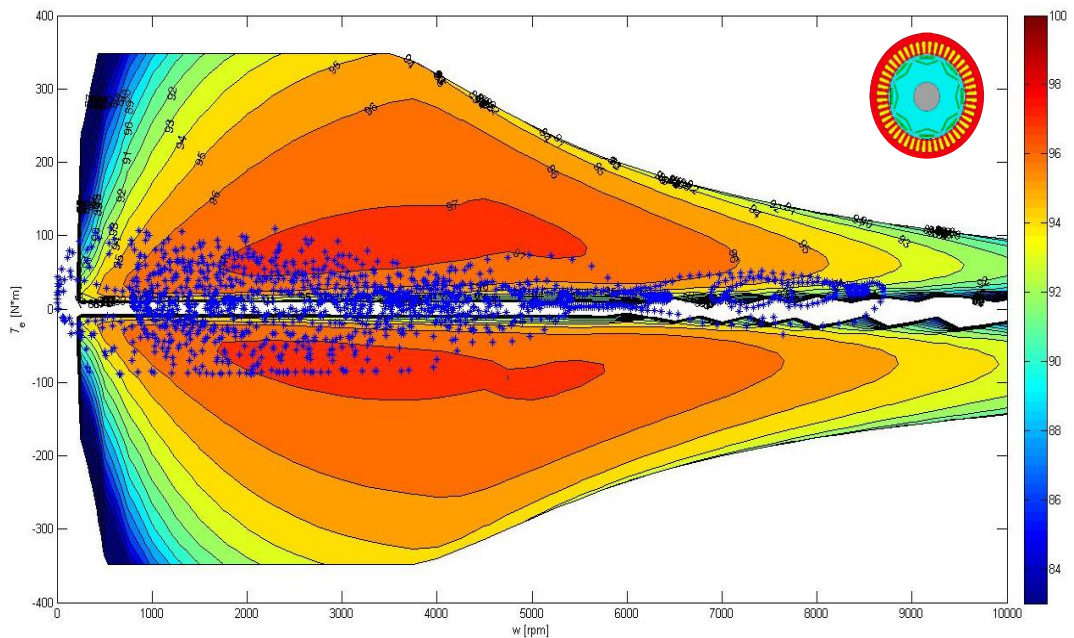
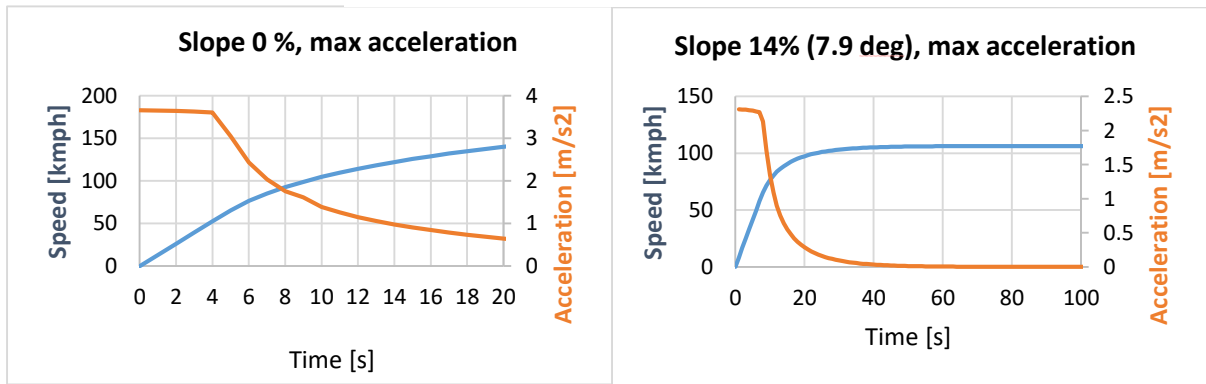


Figure 66 Delta-shape Efficiency



The comparison it has been done following the vehicle performance and the EM average efficiency.

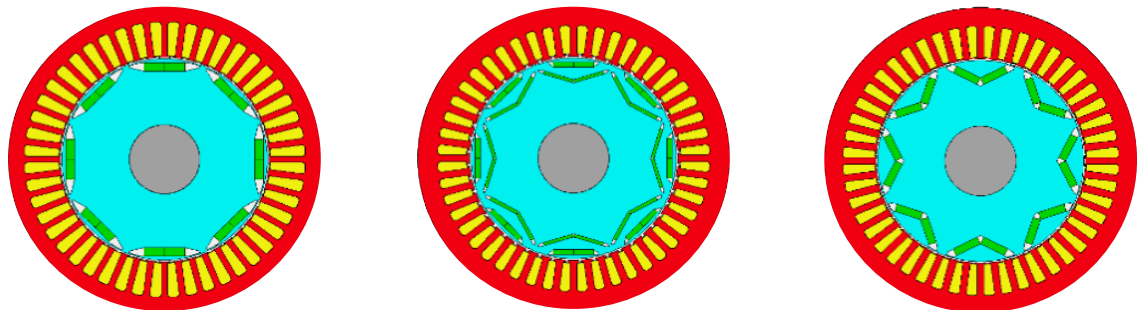
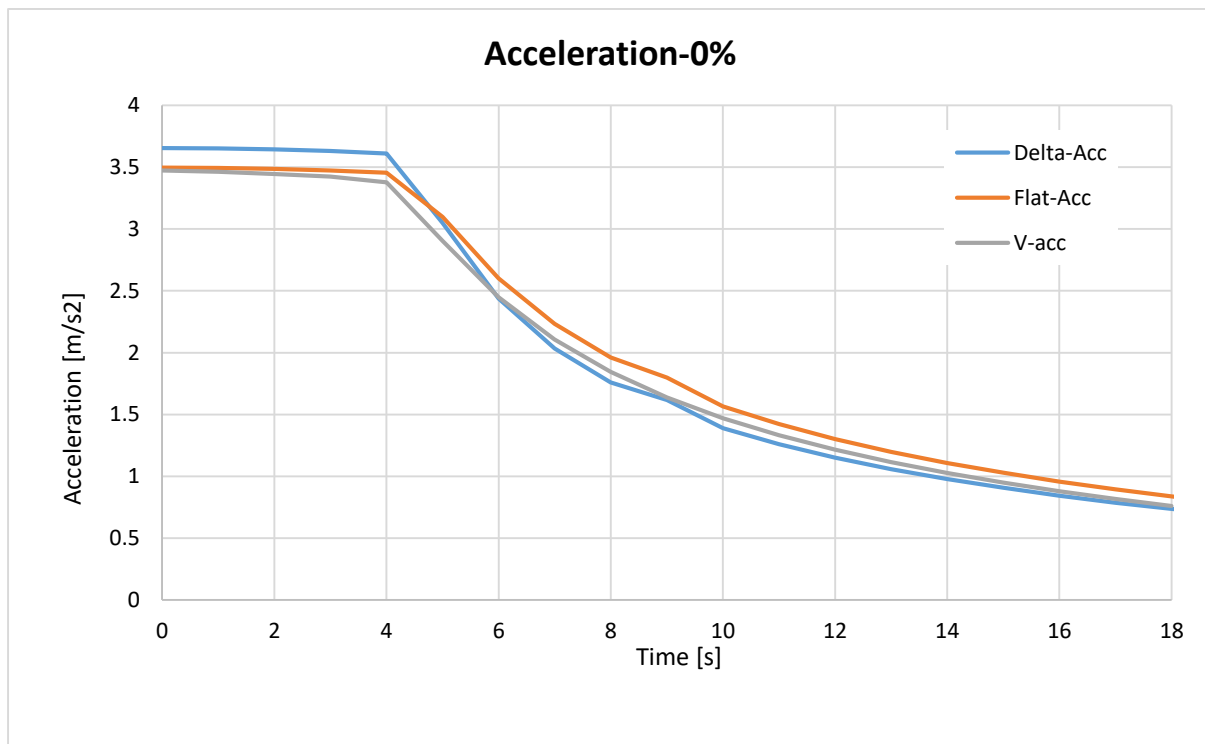


Figure 67 Optimized design



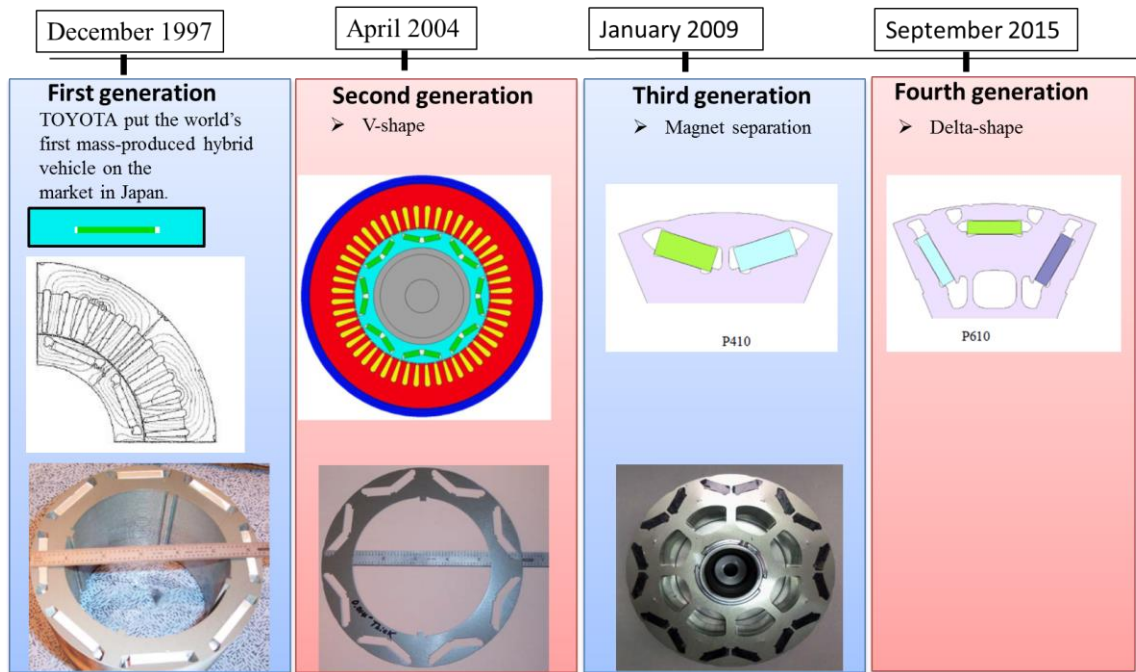
Motor	Unit	Flat	Delta	V
Gear ratio	-	7.5	7.5	7.5
Average efficiency	%	86.9	91.08	87.56
Total loss (WLTP)	Wh	377	233	358

The Delta configuration offer the lowest loss and consequently the best average efficiency.

The next chapter will summarize the results described above in order to give a global view of this thesis.

Chapter 7 Conclusion of the thesis

The purpose of this thesis is describe the evolution of the Permanent Magnet Synchronous Motor in the Automotive world during the last two decades.



The first electric motors were based on flat magnet arrangement, this kind of configuration presents very compact body of the rotor, low production cost due to the fact that the geometry of the section of the rotor is not complicate, but this configuration offer a motor with a very low anisotropic grade (reluctance torque << magnet torque) . This means that the performance of the motor are strongly related to the mass of magnet used and speed range is quite narrow.

In order to decrease the amount of magnet , a strategy to mix the quality of the Permanent magnet synchronous motor was developed with the quality of the Reluctance motor.

Permanent magnet assisted reluctance motors (PMa-SynRM) have been designed to combine the advantages of magnet type and reluctance motors. Since these motors have high power density, high power factor, high efficiency and wide speed range, they become a considerable and popular topic. Because the produced torque is a combination of magnet and reluctance torques, this motor type can be called as a hybrid motor. The rotor can be designed in many different structures to provide both magnet and reluctance torques.

The graph above show the gradual evolution of the EM design in Toyota.

The last picture is not available for confidentiality reason.

Doing a step beyond is possible to see how this design evolution will affect all the powertrain design.

Imagining to start the process for a new electric vehicle development , defined the class of it, will be clear the performance that the car should satisfy :

- Top speed [km/h]
- 0-100 [km/h]
- Max acceleration [m/s^2]
- Max slope [deg]

This process could be represented ideally by a too short blanket that should, in some how , match the request of the clients and of the producers.

Talking about EV the main concern from the client is the driving range. Skipping the new technology related to the battery pack for EV, hence imagining a fix amount of KWh that an EV of this class could install, the producer should find a way to increase the driving range and in the same time define a design of the powertrain that is convenient for a mass production (cost- manutention-durability).

In this contest I have imagined the evolution of the PMSM.

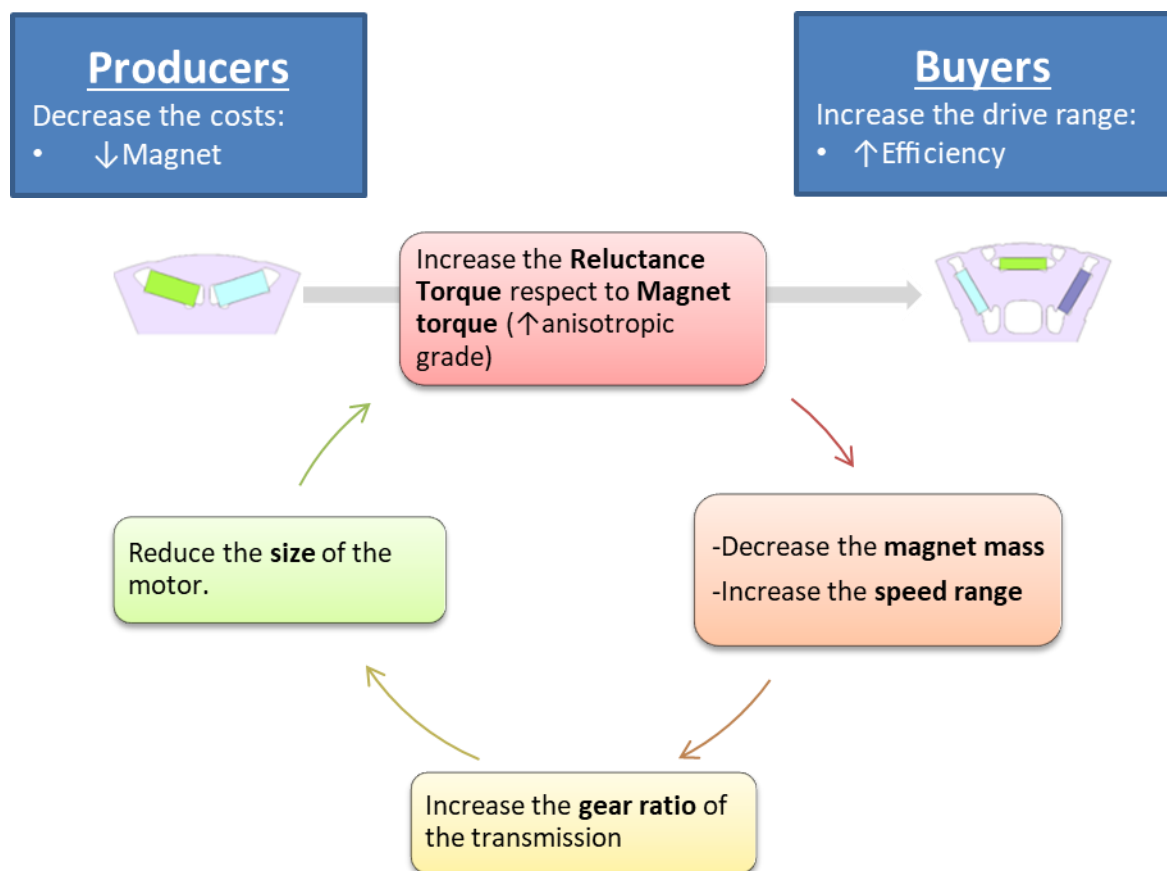


Figure 68 Evolution of PMSM

Bibliography

- [1] J. M. Miller, Propulsion Systems for Hybrid Vehicles. Institution of Engineering and Technology, London, United Kingdom, 2010. [Online]. Available: <http://digitallibrary.theiet.org/content/books/rn/pbrn007e>
- [2] T. D. Gillespie, Fundamentals Of Vehicle Dynamics, 1st ed. Society of Automotive Engineers, Inc., 1992.
- [3] (2014, jan) Density of air. English Wikipedia, the free encyclopedia. Accessed 2014-01-03. [Online]. Available: http://en.wikipedia.org/wiki/Density_of_air
- [4] J. Y. Wong, Ed., Theory of Ground Vehicles, 4th ed. John Wiley & Sons , Inc., 2008.
- [5] W.-H. Hucho, Ed., Aerodynamics of Road Vehicles, From Fluid Mechanics to Vehicle Engineering, 4th ed. Society of Automotive Engineers, Inc., 1998.
- [6] R. B. GmbH, Automotive Handbook, 8th ed. John Wiley Sons, 2011.
- [7] M. Ehsani, Y. Gao, and A. Emadi, Modern Electric, Hybrid Electric, and Fuel Cell Vehicles: Fundamentals, Theory, and Design, 2nd ed. CRC Press, Taylor & Francis Group., 2010
- [8] L. Guzzella and A. Sciarretta, Vehicle Propulsion Systems - Introduction to Modeling and Optimization, 2nd ed. Springer, 2007.
- [9] D. Zarko, D. Ban, T. A. Lipo, "Design Optimization of Interior Permanent Magnet Motor with Maximum Torque Output in the Entire Speed Range", in Proc. Int. Conf. On Power Electronics and Applications 2005, Dresden
- [10] Dr David Staton Dr James "Open Source Electric Motor Models for Commercial EV & Hybrid Traction Motors"
- [11] Plett, Dr. Gregory L. Modeling, Simulation, and Identification of Battery Dynamics. [Online] 2016. <http://mocha-java.uccs.edu/ECE5710/ECE5710-Notes02.pdf>.
- [12] Battery University. [Online] 08 02 2017. http://batteryuniversity.com/learn/article/rising_internal_resistance.
- [13] High Fidelity Electrical Model with Thermal Dependence for Characterization and Simulation. Jackey, Robyn, Gazzarri, Javier and Turan Huria, Missimo Ceraolo. 2012, IEEE.
14. Černá, Ing. Ladislava and Mgr. Jakub Holovský, Ph.D. Electrochemical Sources and Photovoltaics . Lecture extract. Prague, Czech Republic : Faculty of Electrical Engineering, Czech Technical University, 2016.
15. Berg, Helena. Batteries for Electric Vehicles: Materials and Electrochemistry. United Kingdom : Cambridge University Press, 2015.
16. Team, MIT Electric Vehicle. Massachusetts Institute of Technology. [Online] December 2008. http://web.mit.edu/evt/summary_battery_specifications.pdf.

